Annals of Biomedical Engineering, Vol. 47, No. 9, September 2019 *(© 2019)* pp. 1832–1854
https://doi.org/10.1007/s10439-019-02205-4

State-of-the-Art Modeling and Simulation of the Brain's Response to Mechanical Loads

Finite Element Methods in Human Head Impact Simulations: A Review

AMIT MADHUKAR[1] and MARTIN OSTOJA-STARZEWSKI[1,2]

[1]Department of Mechanical Science & Engineering, University of Illinois at Urbana-Champaign, Urbana, IL 61801, USA; and [2]Beckman Institute and Institute for Condensed Matter Theory, University of Illinois at Urbana-Champaign, Urbana, IL 61801, USA

(Received 22 August 2018; accepted 12 January 2019; published online 28 January 2019)

Associate Editor Mark Horstemeyer oversaw the review of this article.

Abstract—Head impacts leading to traumatic brain injury (TBI) present a major health risk today, projected to become the third leading cause of death by 2020. While finite element (FE) models of the human brain are important tools to understand and mitigate TBI, many unresolved issues remain that need to be addressed to improve these models. This work aims to provide readers with background information regarding the current state of research in this field as well as to present recent advancements made possible by improvements to computational resources. Specifically, this has manifested as a drive to introduce more details in FE models in the form of increased spatial resolution and improved material models such as nonlinear and anisotropic constitutive models. The need to work with high-resolution FE meshes is underlined by the dominant wavelengths involved in transient pressure and shear wave propagation and the ability to model the brain surface. We also discuss improvements to experimental validation techniques which allow for better calibrated models. We review these recent developments in detail, highlighting their contributions to the field as well as identifying open issues where more research is needed.

INTRODUCTION

Head injury resulting in traumatic brain injury (TBI) is a leading cause of mortality in the United States, contributing to approximately 30% of all injury-related deaths.[38] Annually, there are approximately 2.8 million cases of TBI-related injuries reported in North America,[131] an increase of almost 65% from 2006.[38] A majority of TBIs are considered to be mild, commonly referred to as mTBIs or concussions.[11,17] Despite this innocuous label, mTBI has the potential to cause chronic cognitive, physical, and psychological disorders.[89,124] In 2003, the Center for Disease Control (CDC) declared TBI to be a "silent epidemic" that requires further study.[17] Clearly, this is a very pertinent issue plaguing humanity for which a great deal of research has been done and still needs to be performed.

This review is structured as follows: "Introduction" provides some background into mTBI as well as the application of finite element models to study its injury pathways. "Material Models of Brain Tissue" introduces and compares the constitutive models proposed to model the mechanical response of brain tissues—a critical component in numerical models. Finally, "Finite Element Modeling of the Human Head" addresses the modeling challenges encountered while creating an accurate numerical model and presents some of the latest models in the field. For reference, we have also included related review articles in the Appendix that readers can explore for further details.

Biomechanics of Concussion

To gain a full understanding on how mechanical impacts cause concussions, we first need insight into how the head responds to motion and how the energy of this motion is transferred to the tissue. The flowchart depicted in Fig. 1, originally published by Ommaya and Gennarelli in Ref. 111 remains one of the clearest depictions of this process.

In this work, we focus on dynamic impacts which can be caused either by impacts—direct blows to the head, especially prevalent in sports-related injuries; or by impulse—a sudden movement of the head, typically seen in car crashes. The injury caused by blast waves is

Address correspondence to Martin Ostoja-Starzewski, Department of Mechanical Science & Engineering, University of Illinois at Urbana-Champaign, Urbana, IL 61801, USA. Electronic mail: martinos@illinois.edu

0090-6964/19/0900-1832/0 © 2019 Biomedical Engineering Society

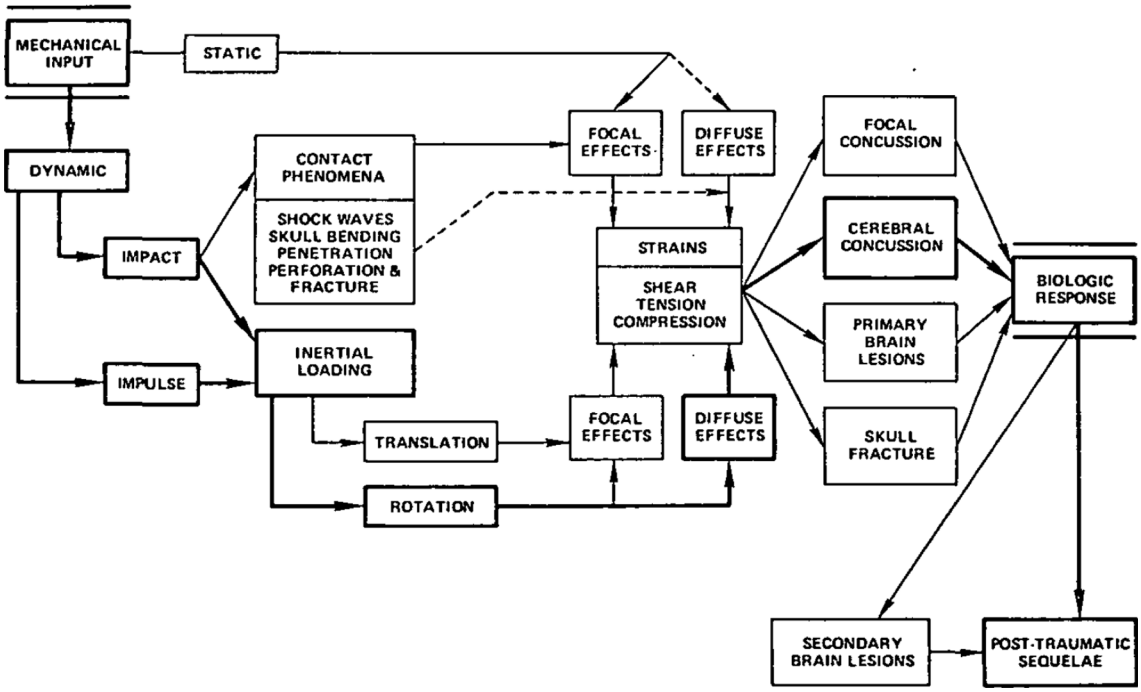

FIGURE 1. Flow chart of primary injury mechanisms caused by mechanical impacts. The mechanical input, often in the form of a dynamic load is shown at the top left. The translational or rotational motion of the head leading to excessive deformation of brain tissue which finally manifests as biological response (from Ref. 111).

not considered here. Instead, interested readers can consult the wealth of research available in this field starting with the recent review papers.[10,42] Dynamic impacts cause inertial loading of the head leading to translational and rotational motion of the head. As is evidenced by clinical studies,[50] brain injury is usually manifested through focal or diffuse effects.

Focal brain injuries are those that are large enough to be observed by the naked eye, caused by translational loading of the brain occurring at the site of contact between the skull and brain. The level of tissue damage correlates directly with the peak pressure achieved during the injury period.[88,63,29] These focal injuries are common in moderate and severe brain injury but are less prevalent in mild TBI (mTBI).[62,1] As such, the rest of this work focuses on diffuse effects.

Diffuse brain injury is associated with more widespread damage to brain tissue, often not easily observable—even with medical imaging techniques, making diagnosis difficult. Diffuse injuries are far more prevalent during rotational motion of the head wherein large shearing forces are applied to brain tissue.[95] Since brain tissue deforms more readily to shearing forces than to compressive or tensile forces,[129,6] diffuse injuries have the potential to be far more damaging than focal injuries of the same impact energy.[111,52,128] Damage to tissue during a diffuse impact is manifested primarily as damage to white matter (more specifically to axon fibers present within the white matter). Diffuse axonal injury, or DAI is the most severe form of cerebral concussion. DAI is one of the most frequent head injuries occurring in almost half of primary intra-axial lesions of the brain,[54,53] and is the second cause of death by TBI.[9] During a diffuse impact of sufficient magnitude, rapid tensile elongation of axons occurs which eventually leads to rupture[132,3] and retraction of axons into "retraction balls".[7] This process is followed by axonal degeneration. While immediate axon rupture is observed in severe brain injury, DAI manifests itself as delayed secondary axon disconnections. Clinical studies show that such injuries are primarily confined to the cerebral white matter,[54,53,7,51,107] with a propensity for lesions in the brainstem and the corpus callosum (*i.e.,* regions with highly organized axon tracts).[5] Damage to these regions is associated with high mortality as these sites serve as vital connection points to other regions of the brain. The rotational motion also causes rotation of the skull relative to the brain, which is likely to tear parasagittal bridging veins and cause subdural hematoma.[16]

Further reading on the topic of the biomechanics of concussion can be found in review papers.[126,98]

Numerical Modeling of the Human Head

Numerical models and, in particular, the finite element (FE) method are extremely useful mathematical tools to determine the mechanical response of brain

tissue during impacts, whether they be focal or diffuse in nature. By discretizing the human head into many smaller elements, the mechanical response of the brain can be approximated as the solution to a system of algebraic equations. The main steps required to create a finite element head model are:

1. Segment and subdivide the head into a finite element mesh, taking care to include all anatomically pertinent features.
2. Assign the appropriate boundary and interface conditions to the mesh. Of particular importance is the skull-brain interface, consisting of the meninges and cerebrospinal fluid (CSF).
3. Assign constitutive models to the elements of the mesh. The constitutive relations chosen should produce a mechanical response that closely mimics biological tissues.
4. Apply loadings to the mesh recreated from real-world scenarios.

Once created, an important final step is to validate the solution computed to existing experiments performed on cadavers. A few popular validation experiments are listed in "Validation with Experimental Data". Once validated for a number of different load cases, results from these models can be extrapolated to study other impact cases.

A review of early finite element models applied to head injury can be found in King *et al.*[79] Restricted by the computational limitations of the time, these crude models were still able to qualitatively agree with experimental results. Since then, research has advanced the field greatly, adding more refinements to the numerical models and removing unnatural assumptions, as described in newer review articles.[146,134,32] In this work we present the latest advancements not addressed by previous reviews, specifically newer models incorporating the anisotropy and nonlinearity of brain tissue, more accurate modeling of the CSF layer and high resolution models capable of capturing wave propagation within the brain. While we focus mainly on the finite element method in this review, other numerical methods have been successfully used to model the human head, two of which we briefly mention here. One of these is the material point method (MPM)[46] wherein the continuum is represented by Lagrangian elements known as 'material points' and a background Eulerian grid is used for solving the governing equations. This background grid does not move and, instead, the material points are convected according to the loads applied. The MPM is considered a mesh-free method since explicit meshing is not required for the material points. As such, it does not suffer from some computational challenges inherent to finite element models such as volumetric locking, convergence issues and severe mesh distortion effects at large deformations. Another numerical method that is primarily used to model fluid-solid interaction is the smoothed-particle hydrodynamics (SPH) method, further discussed in "Modeling of Brain–Skull Interface".

Head Injury Criteria: Or How to Predict Injury Using Finite Element Models

Head injury criteria are measures used to determine the severity of injury following a traumatic event. These criteria are attempts by researchers to link the temporal variation of a single mechanical parameter to the risk of brain injury. Certain parameters such as linear and rotational accelerations are straightforward to measure whereas others such as the maximum principal strain (MPS), the von Mises stress and the intracranial pressure require more complicated experiments to be performed. Finite element models make it possible to perform investigations under conditions not feasible during experiments. Once calibrated, these criteria can be powerful tools to estimate and minimize the chance of injury based on results from simulations or experiments.

The choice of injury criteria is a source of constant debate. Popular injury criteria are the Gadd Severity Index (GSI)[45] and the Head Injury Criterion (HIC).[137] However, these criteria are based on the translational acceleration of the head center of gravity. Zhang *et al.*[149] point out that these criteria neglect the effect of angular acceleration of the head to injury production. Instead, they argue that the predicted shear stress response in the upper brainstem is the best injury predictor over other injury criteria. Yet another injury criterion is the head impact power (HIP).[106] By incorporating the scalar sum of the power terms for all six degrees of freedom, this criteria takes into account both rotational and translational accelerations. Owing to the susceptibility of highly aligned white matter tracts to DAI occurrence, research has been conducted recently to develop injury criteria based on maximal axonal strain (MAS).[57,61,71,59] By incorporating anisotropy into numerical models, it is argued that the strains produced by numerical models are more accurate, leading in turn to more accurate injury criteria based on these strains. Over the years, a large number of other injury criteria have been proposed. The review paper[134] conveniently collects many of these in one place.

MATERIAL MODELS OF BRAIN TISSUE

The brain is one of the softest biological materials exhibiting nonlinear and time-dependent properties. Comprising mostly of water,[96] the bulk modulus of brain tissue is many orders of magnitude larger than the shear modulus, and deformation can be assumed to depend primarily on shear modulus.[149,35] For this reason, determination of shear properties of brain tissue has received considerable attention from researchers. Additionally, brain tissue had a strong strain rate dependence, stiffening as the strain-rate increases.[100,13,118,25] Gray and white matter—the two distinct soft tissues comprising the majority of the brain—have significant mechanical differences. White matter is significantly stiffer than gray matter[149,127,36,34] and, additionally, the presence of myelinated axons renders white matter highly anisotropic, especially in large fiber tracts such as the corpus callosum, corona radiata, and superior longitudinal fasciculus. On the other hand, the gray matter is an isotropic structure.[115]

Constitutive models are carefully constructed approximations of this highly complex behavior of brain tissue. More often than not, compromises are made in some aspects of the material modeling in order to cope with computational constraints. The following sections highlight a large number of constitutive models proposed to describe the tissues of the brain. Unfortunately, there is large variability in data for tissues tested under apparently similar conditions by different research groups. Many review works have provided clarity in the face of this vast mountain of data by collecting and comparing numerical models.[23,19,120] In this section, we attempt to distill the main points of older reviews in the context of impact simulations as well as add new insight into recently popular topics—nonlinearity and anisotropy of brain tissue as well as efforts to accurately capture the CSF.

Linear Material Models

Linear Elastic Model

A linear elastic material model is generally used for hard tissues of the human head, such as skull, scalp and falx/tentorium, where deformation is expected to be very small for the type of impacts leading to mild TBI. Early numerical models utilized elastic materials for the soft tissues of the brain[140,69] due to the simplicity of implementation. However these soft tissues have time-dependent properties, especially in shear, (see "Linear Viscoelastic Models") and as such, elastic material models are inappropriate. Material properties for linear elastic materials used in finite element models are given in Table 1.

Linear Viscoelastic Models

Most numerical models utilize viscoelastic material law for the shear response of soft tissues (white and gray matter, the layers of the meninges and occasionally, the CSF layer). In the linear regime of strain, the viscoelastic response can be captured in terms of a generalized Prony series. The shear relaxation modulus is given by

$$G(t) = G_\infty + \sum_{i=1}^{n} G_i e^{-\beta_i t} \tag{1}$$

where G_∞ is the long-term shear modulus, G_i are shear moduli, and β is the decay constant. Reducing Eq. 1 to one term gives the Kelvin–Maxwell linear model which is often chosen due to the relative simplicity of implementation

$$G(t) = G_\infty + (G_0 - G_\infty)e^{-\beta t}. \tag{2}$$

Commonly used values of these parameters are given in Table 2.

Nonlinear Material Models

Large deformations of soft tissues are often encountered in head impact simulations causing tissue to exceed the linear limit (1% shear strain[113,108]). Outside this limit, nonlinear material models give a more accurate response. The increased computational and implementation expense has meant that these models have come to the forefront only recently.

Mooney–Rivlin Hyperelastic Model

The Mooney–Rivlin hyperelastic model is expressed in terms of the invariants $(\tilde{I}_1, \tilde{I}_2)$ of the isochoric right Cauchy-Green deformation tensor.[1] The strain-energy function is of the form

$$W(\tilde{I}_1, \tilde{I}_2, J) = C_{10}(\tilde{I}_1 - 3) + C_{01}(\tilde{I}_2 - 3) + W_H(J) \tag{3}$$

where J is the relative volume, C_{10} and C_{01} are the Mooney–Rivlin materials constants and W_H is a hydrostatic work term included to eliminate volumetric effects.

[1]If I_1 and I_2 are the invariants of the right Cauchy-Green deformation, the isochoric (or volume preserving) portions are computed as $\tilde{I}_1 = I_1 J^{-1/3}$, $\tilde{I}_2 = I_2 J^{-2/3}$

TABLE 1. Parameters for elastic materials used to model stiff tissues.

Tissue type	Density ρ (kg/m^3)	Young's modulus E(GPa)	Poisson's ratio	References
Skull (as a whole)	2070	6.5	0.20	21
	35200	6.9	0.30	130
	1210	8.0	0.22	148
Dipolë	1750	5.66	0.22	71
	1000	0.56	0.30	147
Cortical bone	3000	15	0.22	71
	2100	6	0.25	147
Dura mater	1130	0.0315	0.45	148,68
Falx	1130	0.0315	0.23	142
	1130	0.0315	0.45	148,68

TABLE 2. Parameters for linear viscoelastic materials used to model soft brain tissues.

Tissue Type	Density ρ (kg/m^3)	Bulk modulus K (GPa)	Short term shear modulus G_0 (kPa)	Long term shear modulus G_∞ (kPa)	Decay factor β (s^{-1})	Ref.
Grey matter	1060	2.19	10.0	2.0	80	139
	1040	0.558	1.66	0.928	16.95	130
	1040	2.19	34	6.4	400	149
	1040	2.19	34	6.4	700	148
	1040	2.278	0.407	0.233	125	72
White matter	1060	2.19	12.5	2.5	80	139
	1040	0.558	1.66	0.928	16.95	130
	1040	2.19	41	7.8	400	149
	1040	2.19	41	7.8	700	148
	1040	2.278	0.407	0.233	125	72
Brainstem	1060	2.19	22.5	4.5	80	139
	1040	0.558	1.66	0.928	16.95	130
	1040	2.19	58	7.8	400	149
Cerebellum	1060	2.19	12.5	2.0	80	139
	1040	0.558	1.66	0.928	16.95	130
	1040	2.190	0.407	0.233	125	72

An extension of the Mooney–Rivlin model was performed by Miller and Chinzei[100] who introduced the strain energy function of the form

$$W(\tilde{I}_1, \tilde{I}_2) = \sum_{i+j=1}^{n} C_{ij}(\tilde{I}_1 - 3)^i(\tilde{I}_2 - 3)^j. \qquad (4)$$

The first two terms in the above (*i.e.*, $n = 1$) give the standard Mooney–Rivlin model in Eq. 3. Through a series of axial compression tests at varying loading rates, they determined that while for low loading rates it was sufficient to use only two terms in the expansion (*i.e.*, C_{01} and C_{10}), this was not the case for larger load rates. To accurately model tissue behavior for a wide range of loading rates, better accuracy was obtained by using four terms (*i.e.*, $n = 2$): C_{01}, C_{10}, C_{02}, and C_{20}. This model was used in the numerical model by Miller *et al.*[101]

Mendis *et al.*[99] specialized the standard Mooney–Rivlin model to brain tissue by introducing rate effects. The modified energy relaxation coefficients are given by

$$C_{10}(t) = 0.9C_{01}(t) = 620.5 + 1930e^{-t/0.008} + 1130e^{-t/0.15} \qquad (5)$$

This modification correctly takes into account the viscoelasticity of brain tissue. Numerical models[68,84] utilize this constitutive model.

Ogden Hyperelastic Model

The more sophisticated Ogden hyperelastic material model is applicable at higher strains than the Mooney–Rivlin model. The strain-energy function can be expressed in terms of the principal stretches $(\lambda_1, \lambda_2, \lambda_3)$ of the right Cauchy-Green deformation tensor as

$$W(\lambda_1, \lambda_2, \lambda_3, J) = \sum_{i}^{3} \frac{\mu_i}{\alpha_i}(\lambda_1^{\alpha_i} + \lambda_2^{\alpha_i} + \lambda_3^{\alpha_i} - 3) + \frac{1}{2}K(J-1)^2 \qquad (6)$$

TABLE 3. Transverse isotropy strain energy formulations used for brain tissue, see Eq. 7.

References	$W_{iso}(\tilde{I}_1, \tilde{I}_2, \tilde{I}_3)$	$W_{aniso}(\tilde{I}_4, \tilde{I}_5)$
Ning *et al.*[109]	Neo-Hookean model: $\frac{G}{2}(\tilde{I}_1 - 3) + \frac{K}{2}(J-1)^2$ where G is the shear modulus, K is the bulk modulus.	Quadratic standard reinforcing function: $\frac{1}{2}\theta(\tilde{I}_4 - 1)^2$ where θ is the strength of the fiber reinforcement.
Velardi *et al.*[136]	1st order Ogden Model: $\frac{2\mu}{\alpha^2}(\lambda_1^\alpha + \lambda_2^\alpha + \lambda_3^\alpha - 3)$ where μ and α are the Ogden material constants.	Ogden-like model: $\frac{2k\mu}{\alpha^2}(I_4^{\alpha/2} + 2I_4^{-\alpha/4} - 3)$ where k measures the increase of stiffness of the material in the fiber direction.
Giordano and Kleiven[58]	Neo-Hookean model: $\frac{G}{2}(\tilde{I}_1 - 3) + K\left(\frac{J^2-1}{4} - \frac{1}{2}\ln(J)\right)$ where G the shear modulus, K is the bulk modulus.	Gasser-Ogden-Holzapfel (GOH) form[48]: $\frac{k_1}{2k_2}(e^{k_2\langle\tilde{E}_\alpha\rangle^2} - 1)$ where $\tilde{E}_\alpha = k(\tilde{I}_1 - 3) + (1-3k)(\tilde{I}_4 - 1)$, k_1 and k_2 are the fiber stiffnesses and k is the dispersion parameter.
Feng *et al.*[41,39]	Neo-Hookean model: $\frac{G}{2}(\tilde{I}_1 - 3) + \frac{K}{2}(J-1)^2$ where G the shear modulus, K is the bulk modulus.	Quadratic function in $\tilde{I}_4$ along with $\tilde{I}_5$ term: $\frac{G}{2}\left[\zeta(\tilde{I}_4 - 1)^2 + \varphi(\tilde{I}_5 - \tilde{I}_4^2)\right]$ where ζ and φ are material constants of the anisotropic model.

where α_i and μ_i are the Ogden material constants. A hydrostatic work term, a function of the bulk modulus K and relative volume J, may be included to eliminate the volumetric effects. This model is tuned by Refs. 108 and 85, among others, for brain tissue. The rate dependence is usually expressed as an N-term Prony series, Eq. 1.

Anisotropic Material Models

While the models considered thus far have been isotropic, brain tissue, especially white matter, is known to be highly anisotropic. Due to the presence of highly aligned axon tracts, transverse isotropy, with the fiber axis normal to the plane of isotropy, is sufficient to describe material response.[109,136,41] Transverse isotropy can be described by the uncoupled strain energy function

$$W = W(\tilde{I}_1, \tilde{I}_2, \tilde{I}_3, \tilde{I}_4, \tilde{I}_5) = W_{iso}(\tilde{I}_1, \tilde{I}_2, \tilde{I}_3) + W_{aniso}(\tilde{I}_4, \tilde{I}_5) \quad (7)$$

where $W_{iso}(\tilde{I}_1, \tilde{I}_2, \tilde{I}_3)$ describes the response of the isotropic matrix; and $W_{aniso}(\tilde{I}_4, \tilde{I}_5)$ describes the directional contribution of the fiber reinforcement. Here $\tilde{I}_1$, $\tilde{I}_2$, and $\tilde{I}_3$ are the standard invariants of the isochoric right Cauchy green deformation tensor, $\tilde{\mathbf{C}}$ while $\tilde{I}_4$ and $\tilde{I}_5$ are two "pseudo-invariants" describing the effect of the fiber reinforcement.[2]

The different models of transverse isotropy used in the literature are presented in Table 3 where a common simplification is to utilize only one invariant ($\tilde{I}_4$) for the anisotropic part. However, it has been shown that at least two anisotropic invariants ($\tilde{I}_4$, $\tilde{I}_5$) are needed to accurately capture the mechanical response of brain tissue[41,31] with the invariant $\tilde{I}_5$ particularly affecting shear deformation.[40] As such, newer models should aim to incorporate both anisotropic invariants.

Fluid-Like Models

Modeling CSF as a Newtonian fluid, though more realistic, is computationally expensive. As discussed later in "Modeling of Brain–Skull Interface" a common simplification is to model the CSF as a soft solid with fluid-like properties. Here we list some often used constitutive models to approximate the behavior of fluids with solid elements

Linear Elastic Solid

The most common approach is to approximate the response of a Newtonian fluid with a nearly incompressible, linear elastic solid. A much larger value of bulk modulus K compared to the shear modulus G allows for nearly incompressible behavior, i.e., a very small change in displacement produces large changes in pressure. For reference, commonly cited values for these constants are: $K = 2.19 \times 10^7$ Pa and $G = 5 \times 10^4$ Pa[153] for a Poisson's ratio of $\nu \approx 0.49924$. Parametric studies have been performed for different values of bulk and shear moduli.[68,72,18,8] In particular, it was determined that modifying these values had a large impact on the principal and shear stress and strains obtained but a lesser impact on the coup pressure.[18]

[2]If $\mathbf{A}$ is the unit vector of the mean fiber direction, then $\tilde{I}_4 = \mathbf{A} \cdot \tilde{\mathbf{C}}\mathbf{A}$; $\tilde{I}_5 = \mathbf{A} \cdot \tilde{\mathbf{C}}^2\mathbf{A}$

Linear Viscoelastic Solid

Another formulation makes use of the Kelvin–Maxwell linear model i.e., Eq. 2 to capture shear relaxation behavior. Both the short and long-term shear moduli are chosen to be much smaller than the bulk modulus of the material to preserve the incompressible limit. A parametric study of various values of these constants is performed by Jing *et al.*[72] who determined that the pressure response obtained during impact was almost identical in all cases. A simplification to the Kelvin–Maxwell model is the Maxwell fluid model where G_∞ in Eq. 2 is set to zero. This material model was used in Refs. 18 and 91 where it was again observed that the material response was insensitive to different values of the short term shear modulus.

Equation of State Model

An equation of state is a constitutive equation that defines the pressure as a function of some state variables. One form used to model fluid behavior is the Mie–Grüneisen equation of state (EOS) where the state variables are the density ρ and the internal energy E_m of the material. This equation of state is linear in energy and can be written in the form

$$p = \frac{\rho_\mathrm{o} c_\mathrm{o}^2 \eta}{(1 - s\eta)^2}\left(1 - \frac{\Gamma_\mathrm{o}\eta}{2}\right) + \Gamma_o \rho_\mathrm{o} E_\mathrm{m} \qquad (8)$$

where ρ_o is the reference density, $\eta = 1 - \rho/\rho_\mathrm{o}$ is the nominal volumetric compressive strain and Γ_o, c and s are material constants. The Mie–Grüneisen EOS model can model the compressible behavior of fluids under conditions of high pressure. This constitutive equation was applied[91,47] for head impact simulations using material properties similar to that of water as a close approximation to CSF behavior.

Choosing a Constitutive Model

The main issue to keep in mind when selecting the constitutive model in an impact simulation is the sophistication of the model—or ability of the model to capture biological features—balanced with its computational cost. For the case of mild impacts, researchers in the past have utilized the linear viscoelastic model to great effect due to the low computational burden.[146] However linear models are ill-suited for the case of impact simulations where large strains and strains rates are expected. Additionally, many of the early experiments from which the properties in Table 2 are determined were performed at low strains or strain rates, some even at quasi-static conditions leading to values that have orders of magnitude difference. These limitations are presented in Table 4 for a few prominent experimental studies and must be kept in mind when selecting a linear viscoelastic model.

The next level of sophistication involves capturing the large-deformation behavior of brain tissue through the use of a hyperelastic material formulation ("Nonlinear Material Models"). Comparisons between many popular models[118,15] have indicated the one-term Ogden hyperelastic model to be best suited to describe the large-deformation elastic behavior of brain tissue. Both the neo-Hookean and the Mooney–Rivlin models assume a linear shear response and, thus, are not capable of capturing the nonlinear shear response of human brain tissue.[15] The modified one-term Ogden model is best able to capture the compression-tension asymmetry when calibrated with all loading modes simultaneously, as seen in Fig. 2.

Since these hyperelastic models are time-independent, researchers often introduce viscoelasticity by assuming the shear relaxation is given by an N-term Prony series. When calibrating the series, it was determined that that the "time-varying shear moduli at the appropriate time scales (e.g., 5 ms and 40 ms corresponding to the impulse durations of the major acceleration peaks for the two impacts, respectively) rather than the initial or long-term shear moduli, were the most indicative of impact-induced brain strains".[150] A more general approach to introduce time-dependence is to decompose the deformation gradient into a time-independent elastic and a time-dependent viscous part, allowing for a fully nonlinear model. These so-called multiplicative decomposition models inherently account for the material response to large deformations and high strain rates.[13,120,70] However, these models require a large number of adjustable parameters and are computationally expensive.

Since axon elongation is the main pathway leading to DAI, many newer models have aimed to model the anisotropy of brain tissue through a constitutive model defined by an uncoupled strain energy functions, "Anisotropic Material Models". Introducing anisotropy strengthens brain tissue in the axon direction and yields more accurate axonal strains. While the work in this field is still ongoing, the research suggest that anisotropy is a crucial detail that should be included in newer models.[57,61]

FINITE ELEMENT MODELING OF THE HUMAN HEAD

The FE method has been used to great effect in modeling dynamic response of brain tissue under impact loadings. In this section, we collect methods from the literature used to construct high-quality numerical models. First, we compare methods used to model the brain-skull interface, an important part of the head

TABLE 4. Experimental studies used to determine material properties of brain tissue along with limitations. Adapted from Ref. 150.

Experiment	Description of experiment; main findings	Limitations	Applications in numerical models
Linear material models			
Shuck and Advani[127]	Dynamic shear experiments conducted on brain tissue up to 350 Hz. Linear, viscoelastic model with two-term Prony series formulated	Limited to strains of 1.3%, even though frequencies are applicable in typical head injury impacts.	21,148,47,135
Mendis *et al.*[99]	Large deformation constitutive model developed to fit existing data. Strain rates up to 40/s considered. Mooney–Rivlin hyperelastic and viscoelastic models developed.	Shear modulus reported found to be overly stiff. Models today use scaled values (10% in Ref. 83).	146,83
Prange and Margulies,[115] Gefen and Margulies[49]	Large strain (50%) shear tests performed on porcine and human brain tissue. First order Ogden model with two-term Prony series derived, later extended to indentation relaxation to derive linear viscoelastic model	Low strain rates of 8.33/s.	28
Finan *et al.*[43]	Microindentation of fresh human brain to determine regional mechanical properties. Gray matter significantly more compliant than the white matter or hippocampus which were similar in modulus. Two- or three-term Prony series linear viscoelastic model applied.	Low strains (0.1) and strain rates (5/s); quasi-static loading	–
Qian *et al.*[117]	Microindentation of porcine brain at varying strain rates and indenter diameter. One- and two-term Prony series linear viscoelastic model applied. Power-law relation for shear modulus with strain rate developed.	Low strain rates (0.2/s); though power-law relation provides acceptable prediction of shear modulus up to 4/s using results from other studies.	–
Nonlinear material models			
Nicolle *et al.*[108]	Oscillatory and shear relaxation experiments performed on human brain tissue for large frequency range. Linear limit of 1% strain determined for brain tissue. Data fitted to third-order Ogden hyperelastic model	Large frequency experiments performed at small strain levels while large strain experiments performed at low frequency	71,85,56
Franceschini *et al.*[44]	Uniaxial quasi-static cyclic tension and compression of brain tissue. Provided evidence that brain tissues obeys consolidation theory. Second-order Ogden hyperelastic model fitted to data	Quasi-static loading	71,82
Jin *et al.*[73]	Large deformation tension, compression and shear tests up to strain rates of 30/s. Gray-white matter heterogeneities and direction dependence also investigated.	Shear relaxation experiments not conducted. No explicit hyperelastic model utilized in the study	–
Rashid *et al.*[118,119]	Dynamic shear, tension and compression tests of porcine brain tissue at large strain rates (120/s). Determined that Ogden hyperelastic model was best-suited to capture response among other hyperelastic models. Two-term Prony series proposed to capture time-dependent response.	Average mechanical properties (mixed white and gray matter) reported.	–
MacManus *et al.*[90]	Indentation experiments performed on mouse brains at large strains (35%) and high strain rates—up to 100/s. Inverse FE analysis performed to fit neo-Hookean, Mooney–Rivlin, and Ogden hyperelastic models	Shear relaxation experiments not conducted; static FE model used in inverse problem to determine hyperelastic material properties	–

model. We then present some experiments that are commonly used to validate these models. Next, we argue for the need to increase spatial resolution of FE models. Finally, we present some cutting-edge models present in the literature; highlighting, along the way, some interesting results obtained from each model.

Modeling of Brain–Skull Interface

Implementation of the brain-skull interface layer is crucial in studying head trauma as it greatly affects mechanical response of the brain.[18,91,110] The constitutive model of these tissues must be chosen with great care. A further consideration is a relative motion

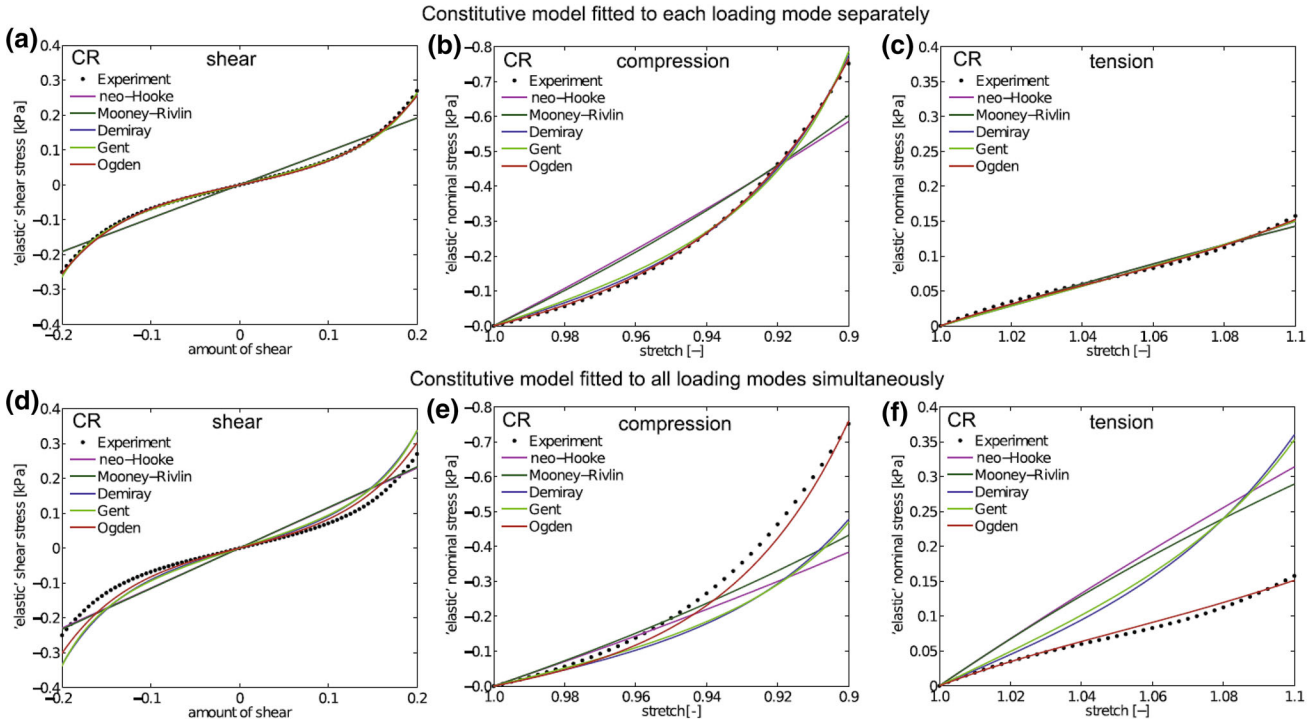

FIGURE 2. Different hyperelastic strain-energy functions (neo-Hookean, Mooney–Rivlin, Demiray, Gent, and Ogden) calibrated against experimental data (black dots). (a)-(c) constitutive models calibrated with data from each loading mode separately; (d)-(f) constitutive models calibrated with data from all loading modes simultaneously. Only the modified one-term Ogden model is able to represent the response of all loading modes simultaneously. (from Ref. 15).

between the skull and brain. Brain motion of Macaque monkeys was recorded under impact using high-speed cinematography, confirming that there is indeed relative motion between the skull and brain.[116] Further experiments determined that most of the intracranial movements occur in the first milliseconds following trauma, indicating strong damping offered by these tissues.[125] Any brain-skull interface model must capture such behavior.

These requirements are satisfied by the CSF modeled as a Newtonian fluid. In a finite element framework, this could be considered by introducing an FSI solver. Willinger and Baumgartner[141] considered an Arbitrary Lagrange Euler (ALE) formulation[65] to model FSI, concluding that the pressure response matched more closely with experimental data for this case than for a solid interface. Toma and Nguyen[133] combined a smoothed-particle hydrodynamics (SPH) approach along with a highly refined FE model to introduce FSI. By clearly meshing the gyri, sulci and ventricular system, they were able to study the cushioning effect of the CSF on these features.

A pragmatic compromise is to utilize a solid formulation that mimics fluid behavior under mild to moderate impacts. Most numerical simulations today follow two approaches to achieve this. The most common approach is to model the CSF as a soft solid material with a low shear modulus. In such a manner, the entire simulation domain can be meshed with solid elements, greatly reducing implementation complexity. Care must be taken, however, to avoid unnatural mesh deformation or mesh entanglement due to elements with very low shear modulus. Different constitutive models have been chosen for such solid material, each having its pros and cons, as detailed in "Fluid-Like Models".

The second approach is representing the brain-skull interface as a frictional surface through contact algorithms. Different strategies are used in order to model the contact conditions, ranging from tied (no slip) to frictionless sliding (free-slip) interfaces. The best choice of contact interface conditions is still up for debate. Kleiven and Hardy[83] performed a parametric study for three types of interface conditions: tied, sliding with separation, and sliding with no separation. They concluded that the tied interface produced solutions that matched experimental data the closest. However, Al-Bsharat *et al.*[2] determined that a sliding interface

performed better. The advantage of the sliding interface is that relative motion is possible between layers.

Often, numerical models combine these approaches—the CSF layer is explicitly meshed with elements using a solid material model, while a contact algorithm between the elements of the CSF and dura/skull allows for relative motion between them. Techniques used to model the brain-skull interface for specific numerical models are presented in "Finite Element Models".

Validation with Experimental Data

Validation of numerical models against experimental data is an important step taken to ensure the model is indeed producing accurate results. There are generally two forms of experimental data available to researchers—intracranial pressure (ICP) or brain displacements. In this section, we look at some popular validation experiments as well as some that have recently been developed.

Nahum et al.'s Impact Experiment

A well-known set of experiments is Nahum *et al.*'s linear impact experiments.[105] A seated cadaver was impacted by a cylindrical impactor weighing $5.59kg$ with a constant velocity of $9.94\ m\ /\ s$. The impact was along the specimen's mid-sagittal plane in an anterior-posterior direction. The skull was rotated such that the Frankfort anatomical plane was inclined 45° to the horizontal, as depicted in Fig. 3a. The resultant input force time history is given in Fig. 3b.

Intracranial pressure history was recorded during the impact event at 5 locations where pressure transducers were placed. This pressure history is utilized in verifying the results obtained from numerical models. Most, if not all, models perform validation with these results. However, it is not sufficient to only validate numerical models against pressure as there is no one-to-one relation between dilatation and distortion—deformation may vary widely in such a way that would not significantly influence the pressure distribution.[14] Since injury mechanisms are caused by deformation, one should view Nahum's results only as an initial validation level in the model development process before validating against a displacement-based method.[97]

Hardy et al.'s Brain Translational Motion Experiment

Brain motion can be captured during impacts using neutral density targets (NDTs). These objects are placed within the cadaver's head and their motion can be captured by high-speed x-rays during an impact. This technique was utilized by Hardy *et al.*[64] to capture the relative displacement data between the skull and brain. In their experiments, the cadaver's head is positioned similar to Nahum's study[105] and translated to an impact speed of $3\ m\ /\ s$ before colliding with a fixed angled acrylic block. Linear accelerations ranging from 38 to 291g was produced. The motion of the NDTs during the impact is captured and recorded. The markers in the brain were observed to follow figure-eight patterns with peak-to-peak excursions as high as 13.4 mm.

Some models which have used these results as validation include[147,83] among others. Validating against brain displacements is beneficial since many brain injury criteria are formulated to account for maximal principal strain or maximal axonal strains.

Alshareef et al.'s Rotational Motion Experiment

Though popular, Hardy *et al.*'s experiments had some key drawbacks. Since the impact was purely

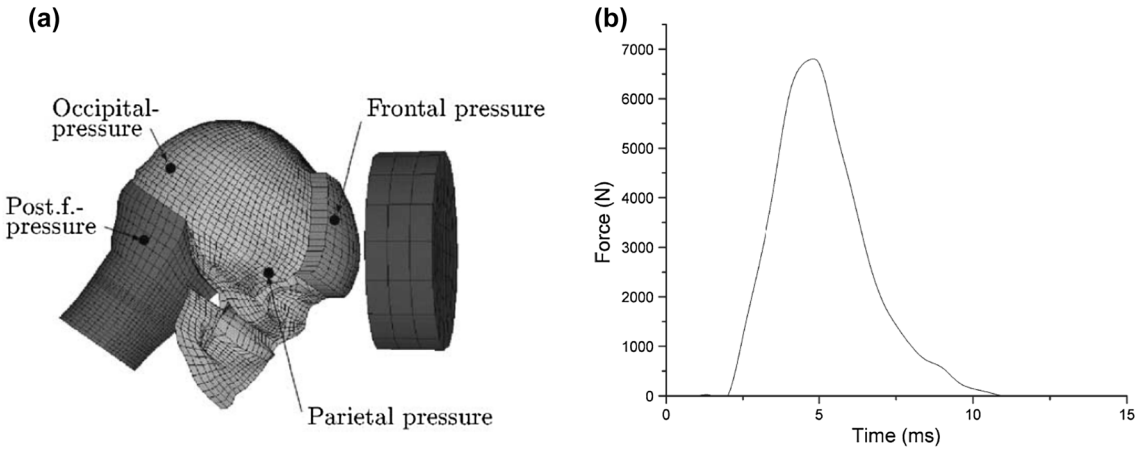

FIGURE 3. (a) Impact location in Nahum *et al.*'s experiments (adapted from Ref. 84). (b) Input force time history (adapted from Ref. 21).

translational, there is very little shearing of the brain tissue. As discussed in "Biomechanics of Concussion", a key injury pathway in DAI is rotational acceleration(s), or diffuse effects. Validating models with focal effects may not be enough when studying DAI. To address this, Alshareef *et al.*[4] performed experiments with the pure rotational loading of the head. Brain motion was recorded with sonomicrometry, a technique which uses ultrasonic pulses to measure the dynamic distances between piezoelectric crystals implanted in any sound-transmitting media. These experiments have the potential to be a more demanding, but ultimately much-needed, verification tool for the next generation of numerical models.

Tagged MRI Experiments

A novel technique to study brain motion *in vivo* is through the use of tagged MRI and harmonic phase (HARP) imaging analysis technique, originally developed for cardiac applications. This technique works by modulating the longitudinal magnetization of the brain tissue in order to create temporary features called tags. These tags serve the purpose of the NDT in previous experiments but here, the process is harmless and reversible. Displacement fields for the *entire* cerebrum can be captured *in vivo* during the impacts, another advantage over previous techniques. This method was utilized to validate brain displacement under mild angular and linear accelerations.[46,122,22] Though these experiments are performed with relatively small deformation magnitudes, they illustrate qualitative features of the brain's response under impacts, which should be captured by any numerical simulation.[122]

Need for High Resolution Models

As greater computational resources become available, it is possible to greatly increase the geometric complexity of head models. We present two arguments in favor of improving spatial resolution, both of which result in more accurate responses.

The first is that high-resolution models are a prerequisite if one is interested in studying the role of stress wave propagation in TBI. In order to properly resolve the high-frequency waves generated during impacts with sufficient accuracy, a minimum number of elements are required per wavelength of the wave. A quick estimation of this metric can be determined from simple wave motion:

Consider the loading in the form of a propagating harmonic wave

$$u(x,t) = A \cdot \sin\left[\omega\left(\frac{x}{c} - t\right)\right],$$

where A is the amplitude and f a waveform propagating at a speed c for a wavenumber k. Here, as always in wave motion, we have $\omega = kc$ and $k = 2\pi/\lambda$, so that the wavelength $\lambda = Tc$, where T is the wave's period. Thus, for longitudinal (pressure) and transverse (shear) type waves, respectively, $\lambda_{\mathrm{L}} = Tc_{\mathrm{L}}$, $\lambda_{\mathrm{T}} = Tc_{\mathrm{T}}$.

It follows that, for a loading period $T \simeq 10\,\mathrm{ms} \equiv 10^{-2}s$ (such as in Nahum's experiment[105]) and brain tissue's typical wave speeds $c_{\mathrm{L}} = 1.5 \times 10^3$ m/s and $c_{\mathrm{T}} = 5$ m/s, we have

$$\lambda_{\mathrm{L}} = 15\ \mathrm{m}, \quad \lambda_{\mathrm{T}} = 5\ \mathrm{cm}.$$

Bradshaw and Morfey[14] suggest a minimum of 10 elements per wavelength. Thus, an element size of 5 mm is required to adequately resolve the potentially more damaging shear waves. For loadings lasting 10^{-3} s or less, this requirement becomes even more stringent. A coarse FE mesh (with elements with size on the order of 1 cm) may be adequate for pressure waves but is totally inadequate for shear waves. Thus, the more transient the loading, the finer must the FE mesh be.

The second argument for increasing spatial resolution is the ability to accurately model the intricate folding of the brain surface, i.e., gyri and sulci. In many models the brain surface is modeled as a smooth surface surrounded by a uniform layer of CSF. However, this simplification results in vastly different stress and strain responses close to the brain surface[27,67] and hence, surface tissue-based injury criteria should not be applied to such simplified models. Since the pia matter adheres to the brain, even within the sulci, it is speculated that stiffness is increased tangential to the cerebral cortex on the inclusion of sulci. Ho and Kleiven[67] demonstrated that inclusion of sulci altered the strains observed by as much as 28% in some regions—making the inclusion of sulci a very pressing concern for future FE head models.

Finite Element Models

Early FE models, often limited by computational resources, attempted crude approximations of anatomical features. Two-dimensional models utilized the plane strain and antisymmetric assumptions in an effort to simplify the model geometry.[121,24] In recent years, three-dimensional models have become increasingly more realistic with the inclusion of greater level of detail in model geometry. Fine features such as bridging veins, brain vasculature and other details of the meninges layer; the complicated folding sulci and gyri of the cerebral cortex; as well as the inclusion of the cavities of the ventricular system are some examples of these improvements. Motivated by the argu-

TABLE 5. Prominent finite element head models used for head impacts in recent years. Dates represent publication of latest improvements to each model.

References	Year	# of elements	Model description
Viano *et al.*[139,80]	2003	314,500	Latest version of the WSUBIM, detailed in "WSU Head Model". Skull, scalp, dura, falx cerebri, tentorium, pia, sinuses, CSF, cerebrum, cerebellum, brainstems, ventricles and bridging veins modeled. CSF modeled with solid elements with a nearly incompressible, elastic model. Low-friction slip contact algorithm used to allow for sliding between the brain and the dura layer.
Willinger and Baumgartner[141]	2003	16,824	An updated version of the SUFEHM, segmented into scalp, skull, CSF, tentorium, flax, brain and brainstem. Bridging veins and vascular system are absent. The elastic-brittle constitutive law implemented to simulate fractures of the skull. Anisotropy of white matter considered by Sahoo *et al.*[123] through the anisotropic constitutive model.
Horgan and Gilchrist[68]	2003	9000–50,000	High-quality, reconfigurable model with easy remeshing capabilities. Crude sections are identified from CT datasets within which mesh density can be varied as needed. Scalp, 3-layered skull (outer and inner tables, diploe), dura, CSF, pia, falx, tentorium, cerebral hemispheres, cerebellum and brainstem captured. CSF modeled as linear elastic solid. Yan and Pangestu[144] modified the original model by replacing CSF formulation with a hydrostatic fluid cavities by using a surface-based technique. Modified model yields more accurate results.
Takhounts *et al.*[130]	2008	45,875	An updated version of SIMon head model. Optimized for fast run-times while matching available head-crash experimental data. Cerebrum, cerebellum, brainstem, ventricles, combined CSF and pia arachnoid complex layer, tentorium and major blood vessels included. To reduce computational cost, shell elements are used to model the skull, falx cerebri, and tentorium
Ying and Ostoja-Starzewski[21]	2010	1,061,799	High resolution model, detailed in "Ying and Ostoja-Starzewski Head Model". MRI data sets used to convert image voxels directly to hexahedral elements with element size of 1.33 mm $\times$ 1.33 mm $\times$ 1.30 mm—identical to the image resolution. Segmented into scalp, skull, CSF, gray matter and white matter with CSF modeled as linear elastic solid, viscous Maxwell fluid and a Mie–Grüneisen equation of state (EOS) model. Realistic distribution of CSF within the ventricular system, the folding structure of the surface of the cerebral cortex and differentiation of gray and white matter within the cerebrum and cerebellum are achieved. Possible to capture propagation of pressure and shear waves. Detailed in "Yang *et al.* Head Model".
Mao *et al.*[93]	2013	270,552	GHBMC head model recreated using a multi-block approach.[92] The final model integrated with neck, thorax, abdomen, pelvis, and lower extremity to form whole body model intended for car-crash simulations. Includes the cerebrum, cerebellum, brainstem, ventricles, bridging veins, CSF, skull, facial bones, meninges, falx and tentorium. Linear viscoelastic constitutive model was chosen for the tissues of the brain, CSF and face while other tissues were modeled as linear elastic.
Kleiven *et al.*[61,84,83]	2014	21,345	KTH finite element head model, detailed in "KTH Head Model". Includes skull, facial bones, scalp, cerebrum, cerebellum, dura matter, flax and 11 pairs of bridging veins. CSF layer modeled as membrane elements with a linear, nearly incompressible elastic solid. Dura matter in tied contact with scalp and sliding contact with the CSF layer. Refined model by Ho and Kleiven[67] with a minimum element size of 1 mm^3 includes sulci and gyri, refined delineation of gray and white matter. Giordano and Kleiven[58] included anisotropy with a hyperviscoelastic, fiber-reinforced constitutive law.
Tse *et al.*[135]	2014	1,337,903 tetrahedral elements	Detailed model of an entire human head with facial bone features, teeth, cervical vertebrae, nasal septal cartilage, nasal lateral cartilages; brain components such as cerebrum, cerebellum, brainstem and CSF. Soft tissue overlaying skull and nasal cartilage also included. Linear tetrahedral mesh generated with average size of 1.57 mm. CSF layer modeled as linear elastic solid material; contact conditions of tangential sliding interface condition applied between skull and the CSF boundary condition, with the coefficient of friction of 0.2
Yang *et al.*[145]	2014	1,173, 039	Model of the 50th percentile Singapore Chinese male segmented with both intracranial features such as cerebrum, cerebellum, CSF, ventricles and spinal cord as well as extracranial tissues like cartilages, fats, and neck muscles. Linear viscoelastic constitutive model utilized for brain tissues. CSF simulated by surface-based fluid modeling method.
Zhao and Ji[152]	2015	115,200	Updated version of Dartmouth Head Injury Model (DHIM) for the entire head. Exterior components including facial bones, mandible, teeth, eye and scalp explicitly modeled. Intracranial components such as cerebrum, cerebellum, falx, tentorium and brainstem modeled with hexahedral elements. One layer CSF represented as soft elastic elements with sliding contact with between skull. Anisotropic fiber strains computed by Ji *et al.*[71] and Zhao *et al.*[151]

TABLE 5. continued

References	Year	# of elements	Model description
Johnson *et al.*[74]	2016	2,578,464	High-resolution model of the entire human head used to solve the optimization problem for helmet facemask design during impacts. Exterior components such as facial bones, mandible, eyes, nose, *etc.* captured from MRI datasets. Tied contact algorithm used for CSF-brain interface. Observed that peak head acceleration was not a good indicator of pressure or shear strain in the brain, making it inaccurate as a head injury criteria. Detailed in "Johnson, Horstemeyer *et al.* Head Model".
Garimella and Kraft[47]	2016	153,328	Embedded element method utilized to couple axonal fiber tractography with volumetric elements. Brain tissue, or matrix, modeled as Mooney–Rivlin hyperelastic; axonal fibers as Ogden hyperelastic material. Detailed in "Anisotropic Head Models".
Ghajari *et al.*[56]	2017	$\sim$ 1,000,000 hexahedral elements; 250,000 quadrilateral elements	Model generated from MRI data sets (1.75 $\times$ 1.75 $\times$ 2 mm^3 voxel size) segmented into scalp, skull, brain, meninges, subarachnoid space and ventricles. Sulci, gyri and ventricles were also included. A two-term Ogden hyperelastic model with a six-term Prony series applied for brain tissue while CSF modeled as a one-term Ogden material without any time-dependence. Inclusion of accurate sulci geometry allowed for a detailed study of injury occurrence to these regions during three impact cases.
Miller *et al.*[102]	2017	2,122,232	Atlas-based Model (ABM) with high-resolution mesh captured by directly converting MRI voxels to hexahedral elements. Cerebrum (combined gray and white matter), cerebellum, CSF and ventricles segmented automatically with the flax and tentorium manually added. Sulci and gyri of the cerebrum as well as ventricles modeled. Kelvin–Maxwell viscoelastic model determined for brain tissue by optimizing model response vs. multiple impact experiments. Detailed in "Atlas-Based Brain Model".
Toma and Nguyen[133]	2018	156,137	Smoothed-particle hydrodynamics (SPH) method to simulate FSI. High resolution model captures gyri, sulci and ventricular system, allowing for the study of cushioning effect of the CSF on these features.

ments in the previous section, we present some models developed recently that showcase high spatial resolution. Additionally, we describe recent updates to some popular models while we list many others developed in the past two decades in Table 5. Older models covered in other review articles[146,134,32] have not been covered in much detail.

KTH Head Model

The numerical head model by Kleiven *et al.*[61,84,83] known as the Kungliga Tekniska Hogskolan (KTH) head model, is one that has seen considerable development. The latest version of the model[61] has 21,345 elements and captures the skull, facial bones, scalp, cerebrum, cerebellum, dura matter, flax and simplified brainstem and neck. The finite element mesh is a mixture of 4-node shell elements to model the skull, facial bones, and scalp; 8-node brick elements for the soft tissues of the cerebrum, cerebellum, and brainstem; and 4-node membrane elements for the dura matter, tentorium and falx. In this way, the model is able to approximate complex anatomical features at a relatively low computational cost.

The skull-brain interface was approximated by the dura matter, which is in tied contact with the scalp and sliding contact with the CSF layer. The CSF layer was approximated as membrane elements with a linear, nearly incompressible elastic solid. An improvement of the numerical model was presented in Ref. 66 by modeling the highly convoluted vasculature within the brain as 5mm long beam elements. A further improvement of the head model was performed by decreasing the element size to around $1mm^3$ allowing for the inclusion of sulci and gyri.[67] It was determined that inclusion of these features changes strains within the head. Anisotropy of white matter was included in the latest versions of the model, known as KTH ANISO[61,59] (see "Anisotropic Head Models"). A comparison of the isotropic and anisotropic versions of the KTH model revealed that the latter performed better when compared to experimental impact response.[60]

WSU Head Model

Another popular model is the Wayne State University Brian Injury Model (WSUBIM). The cur-

rent revision[139,80] consists of 314,500 elements and includes the skull, scalp, dura, falx cerebri, tentorium, pia, sinuses, CSF, cerebrum, cerebellum, brainstems, ventricles and bridging veins. The CSF was modeled with solid elements with a nearly incompressible, elastic model and a low-friction slip contact algorithm was used to allow for sliding between the brain and the dura layer. Additionally, MRI and CT data sets were utilized to recreate a realistic model of the face with 14 bones and 36,400 elements. The detailed face model allowed for simulation of nasal bone impacts where a damage model was included for the bony material using a distortion energy failure criterion.[147] Mao *et al.*[92] developed an efficient method of generating high-quality all-hexahedral finite element meshes using the multi-block approach allowing mesh density to be adjusted easily.

GHBMC Head Model

The Global Human Body Model Consortium (GHBMC) head model[93] was recreated using a multi-block approach as described in Ref. 92. The final model has 270,552 elements and is integrated with other body component models to form a whole body model intended for car-crash simulations. The model includes the cerebrum, cerebellum, brainstem, ventricles, bridging veins, CSF, skull, facial bones, meninges, falx and tentorium. A tied contact algorithm was used between the dura and the arachnoid layers to ensure stability of the model. A linear viscoelastic constitutive model was chosen for the tissues of the brain, CSF and face while other tissues were modeled as linear elastic. The model was validated against a large number of experimental studies, showing good predictive capabilities.

Ying and Ostoja-Starzewski Head Model

Ying and Ostoja-Starzewski[21] used MRI data sets to convert image voxels directly to hexahedral elements with an element size of 1.33 mm × 1.33 mm × 1.30 mm—identical to the image resolution—leading to a mesh of 1,061,799 elements. The MRI voxel-based approach offers a more accurate and complete rendering of the head than other methods where voxels are interpolated onto a coarser mesh, leading to some loss of anatomical accuracy. The model is segmented into scalp, skull, CSF, gray matter and white matter. The CSF was modeled initially as a linear elastic solid and extended to a viscous Maxwell fluid and a Mie–Grüneisen equation of state (EOS) model.[91] Fine anatomical features such as membranes, bridging veins and vascular network were neglected in the initial model. To compensate, a larger value of shear stiffness was assigned to the CSF layer. Joldes *et al.*[76] added the falx cerebri as well as other meningeal membranes to the model by carefully reassigning elements from the CSF, gray and white matter sets based on geometry observed in MRI scans. It was found that inclusion of these features improved the predictive capability of the model. An MRI-based validation of the model was reported in Ref. 22. A 2cm head drop was observed to cause 2-3mm displacement in the brain.

The model is able to capture the folding structure of the surface of the cerebral cortex as well as give a realistic distribution of CSF within the ventricular system and differentiation of gray and white matter within the cerebrum and cerebellum. A drawback of this technique is the tendency to produce jagged edges on mesh surface and material interfaces, which could result in numerical errors. Thus, a mesh smoothing algorithm was applied to obtain a satisfactory finite element mesh.

The fine mesh resolution of this model allows for such a study where it is observed that blunt impacts give rise not only to a fast pressure wave but also to a slow, and potentially much more damaging, shear wave that converges spherically towards the brain center.[91] Details of this convergent shear wave are dependent on the modeling of the skull-brain interface, whereas the peak pressure is not as significantly affected. Due to the sensitivity of brain tissue on shear strains, this convergent shear wave could be a key factor in diffuse injuries observed during TBI; a similar phenomenon was reported in Ref. 87. On a separate track, motivated by the fact that human brains possess fractal geometries,[81,78] a study of acoustic-elastodynamic interactions in spherical geometries was reported in Ref. 77.

Yang et al. Head Model

A high-resolution head model consisting of 1,173,039 elements was developed by Yang *et al.*[145] to model the 50th percentile Singapore Chinese male. In addition to direct segmentation of cerebrum, cerebellum, CSF, ventricles and spinal cord from MRI data sets, extracranial tissues like cartilages, fats, and neck muscles are also included through manual segmentation. Linear viscoelastic constitutive model was applied to the soft tissues of the brain. The CSF was simulated as a hydrostatic fluid filled in cavities by using a surface-based fluid modeling method (previously utilized by Ref. 144). This approach allows for fluid-solid interaction without the need of any elements, avoiding any issues that may arise due to excessive mesh distortion. The head model has been verified by both Nahum's intracranial pressure and Hardy *et al.*'s displacement results.

Atlas-Based Brain Model

The Atlas-Based brain model (ABM) developed by Miller *et al.*[102] is another high-resolution model created by the directly converting MRI image voxels to hexahedral elements. The final mesh consists of roughly 2 million elements segmented into the cerebrum (combined gray and white matter), cerebellum, CSF and ventricles with the flax and tentorium manually added. While mesh smoothing was not performed to remove jagged edges, unusual strains were not observed at material boundaries. The high spatial resolution allows the ABM to resolve the sulci and gyri of the cerebrum as well as the complex structure of the ventricles.

The ABM was used to determine optimal material parameters for the Kelvin–Maxwell linear viscoelastic model of brain tissue by comparing the model response to impact experiments. Error between the observed and predicted response was quantified using CORrelation and Analysis (CORA), allowing for an objective way to quantify error and optimize material parameters. In this manner, the material parameters for brain tissue that produce the highest average CORA score for all the impact cases considered is determined. The strongest relationships between CORA and material parameters were observed for the shear parameters, foremost of which was the short term shear modulus, G_0. The CORA score was also used to compare many popular methods[103] where the KTH model achieved the highest average CORA rating while the ABM received the highest average rating among the different impact cases.

Johnson, Horstemeyer et al. Head Model

Johnson *et al.*[74] developed a head model that utilizes brain injury metrics (tensile pressure and shear strain) as objective functions in a design optimization study. Their model, which contains roughly 2.5 million elements, captures the entire human head including extracranial features such as cartilage, skin and facial bones. The optimal design of a football helmet facemask was determined by minimizing the maximum tensile pressure and shear strain in the brain under impact loadings. Due to the prohibitively large cost of a single impact simulation, surrogate modeling[138] is used to perform the optimization. By performing a Design of Experiments (DOE) study, the surrogate model is trained with only 10 simulations and this surrogate model (which executes in a matter of seconds or less) becomes the basis for further optimization. This study gives a unique application of finite element head models that has scope for large reductions in concussion risk in sport-related injuries.

Ghajari, Hellyer and Sharp Head Model

A high fidelity model of the human head was generated from MRI data sets ($1.75 \times 1.75 \times 2\ \text{mm}^3$ voxel size) of a healthy 34-year old male.[56] The model consists of nearly one million hexahedral elements and a quarter of a million quadrilateral elements, segmented into scalp, skull, brain, meninges, subarachnoid space and ventricles. Sulci, gyri and ventricles were also included in the model. A two-term Ogden hyperelastic model with a six-term Prony series was applied to model brain tissue. The CSF was modeled as a one-term Ogden material without any time-dependence. The inclusion of accurate sulci geometry allowed for a detailed study of injury occurrence to these regions during three impact cases. The model predicted large strains occurred more regularly at the depths of sulci. The volume fraction of sulcal regions exceeding principal strain injury thresholds was significantly larger than that of gyral regions. These results provide further evidence that inclusion of sulci affects model response (Fig. 4).

Anisotropic Head Models

Tensile elongation of axons leading to DAI is a crucial injury pathway that numerical models should aim to predict. It has been shown that shear stress and strain are the main predictors for DAI injury.[80,104] As is evident from previous discussion, the mechanical response of brain tissue is highly dependent on its underlying neuroarchitecture. White matter tissue is highly anisotropic due to the presence of aligned myelinated axons. Incorporating this anisotropy into finite element head models is one area that has seen considerable development in recent years in an attempt to more accurately predict DAI risk. Here we list some popular methods used to inform the numerical methods of the anisotropy present in brain tissue.

One popular method is to map the Fractional Anisotropy (FA)[3] values determined by DTI data sets onto elements of the mesh as a post-processing step. This approach was applied to the SUFEHM head model by Refs. 123 and 20. Due to the difference between the resolution of the imaging voxels and the element size, a weighting function is used to average the FA of multiple voxels coinciding with a single element. The isotropic version of the SUFEHM is then used to compute the strain tensor over each element and a post-processing step is needed to compute the strains in the direction of axons (by transforming the

[3]Amount of anisotropy is expressed as Fractional Anisotropy (FA), a scalar that represents the restriction of diffusion to one axis; zero being unrestricted and one being fully restricted, i.e., totally anisotropic.

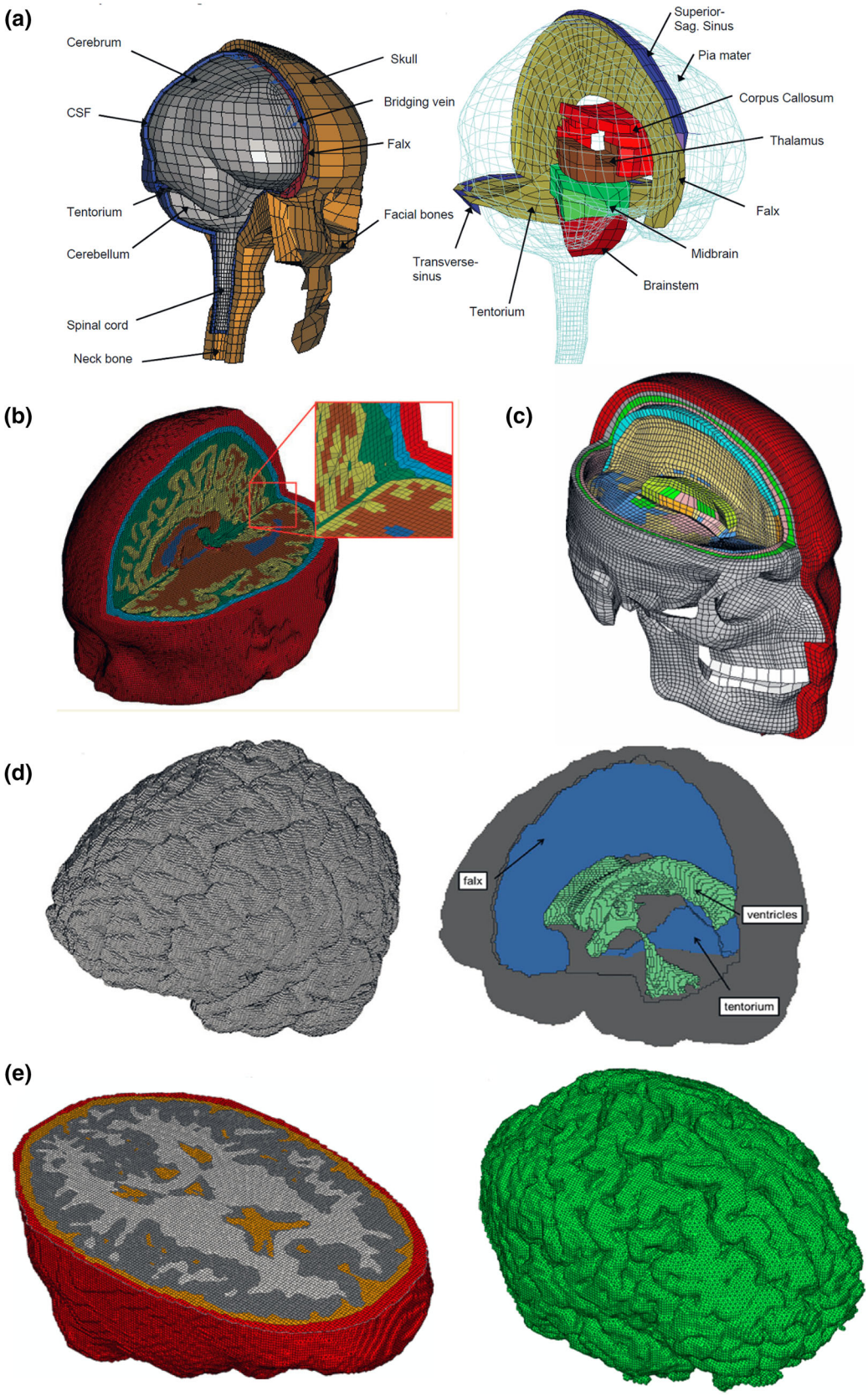

FIGURE 4. Various finite element models reviewed in this work. (A) KTH head model.[85] (B) Ghajari, Hellyer and Sharp Head Model.[56] (C) GHBMC head model.[93] (D) ABM[102] (E) Ying and Ostoja-Starzewski head model.[21]

strain tensor in the direction of axon alignment). The axonal strain computed this way is thus informed by element anisotropy. However, a potential drawback of this weighted-averaging technique is the loss of axonal strain information leading to loss of numerical accuracy. Other numerical models utilizing this technique can be found in Refs. 86 and 143. Work by Refs. 71 and 151 refined the modeling by removing the need for averaging—thereby improving the accuracy of the fiber network resolved by the numerical model.

The approach above, while demonstrated to improve the predictive capabilities of the numerical model, still utilizes an isotropic material model for the brain tissue. The element strains computed from such models are therefore potentially less accurate. A remedy is to consider an anisotropic material model for the white and gray matter. This approach is investigated in Refs. 59 and 58 where a hyper-viscoelastic, fiber-reinforced anisotropic constitutive law is chosen based on the model from Ref. 26. This constitutive model is detailed in "Anisotropic Material Models". Utilizing a weighted-average FA value to directly inform the constitutive model over each element, axonal strains computed using this method should be more realistic. Giordano and Kleiven[58] determined that fiber orientation plays an important role in determining the stress computed for the element. When fibers are mainly perpendicular to the direction of loading, they cannot take part in the stress transfer and smaller stresses are seen together with larger stretches. The opposite is true when fibers are aligned in the direction of the force.

A third approach to introduce anisotropy is the embedded element method, first developed by Refs. 112 and 12. Garimella and Kraft[47] applied this method to study TBI wherein the fiber network computed from DTI data sets was converted to a mesh of truss elements and incorporated into the brain mesh. Using the embedded element model, the translational degrees of freedom of the embedded fibers were constrained to the interpolated values of the corresponding degrees of freedom of the host element. In this way, white matter tracts are explicitly modeled by the finite element mesh and axonal strains can be directly evaluated without the need for post-processing steps. Additionally, the fiber network can be captured with a high level of accuracy without the need for averaging. The final embedded element model contained 153,328 hexahedral elements for the skull, CSF and brain and 161,881 truss elements for the fiber network with an average length of 44 mm.

In all cases, the axonal strains computed using these anisotropic numerical models were significantly different than other measures of strain, such as the von Mises strain and the maximum principal strain. For instance, Giordano *et al.*[57] observed that, within the corpus callosum, the maximum axonal strains are significantly lower than the maximum principal strains for both the isotropic and anisotropic constitutive models. In other words, the principal strain is an overprediction of the axonal strains for brain tissue. Since axon extension is a direct contributor to DAI, the axonal strain was found to be a better injury predictor than predictors using other measures such as angular acceleration or maximum principal strain.[61]

CONCLUSION AND OPEN ISSUES

In this work, we presented a review of the current state of research in head injury models. The complex structure and composition of the human brain pose many challenges to researchers attempting to understand the nature and extent of injury caused by mechanical impacts. The use of numerical methods, and particularly the finite element method has led to great advances in this field, providing a valuable tool for predicting the occurrence of brain injury. We provided a detailed review of the techniques used to create high-quality numerical models from the constitutive models, interface conditions as well as the meshing of the human brain. Additionally, we presented experimental studies often used to validate these models.

Despite the progress made over the past two decades, there is much scope for improvement. We list some open issues that should be addressed by future research:

- With increasing computational resources, the resolution of finite element models should be increased to model finer features and provide more accurate delineation of material boundaries. Direct conversion of imaging voxels to elements has been demonstrated to provide high-resolution models.
- The modeling of the CSF layer can be improved by introducing more realistic material models. Additionally, fluid-solid interaction models can be considered for the next generation of head models.
- Local differences in mechanical properties within the white matter needs to be accounted for. Magnetic Resonance Elastography (MRE) is a novel tool that is able to capture these heterogeneities non-intrusively, as demonstrated by Ref. 75.

- Finite element models are capable of estimating DAI risk by computing instantaneous stress and strain response immediately after an impact. However, the major damage of DAI is delayed secondary axon disconnections which develops over a long time. History-dependent damage models should be considered to study the evolution of injury over a longer time period, as explored in Ref. 55.

APPENDIX A: LIST OF RELATED REVIEW ARTICLES

Here we list related review articles—in chronological order—that the reader may find interesting to explore further.

1. King *et al.* (1995): Review of early finite element models used in impact studies.[79]
2. Nigel A. Shaw (2002): Detailed review of neurophysiology of concussion.[126]
3. Doblaré *et al.* (2004): Computational modeling of bone fracture and healing.[33]
4. Yang *et al.* (2006): Compilation of numerical models, including head models, used in car-crash analysis.[146]
5. Cheng *et al.* (2008): Rheological properties of tissues of the central nervous system.[23]
6. Chatelin *et al.* (2010): Comparison of *in vivo* and *in vitro* techniques used to characterize brain tissue.[19]
7. Meaney and Smith (2011): Introduction to the biomechanics of concussions.[98]
8. Bass *et al.* (2012): Brain injuries arising from blast waves.[10]
9. Meaney *et al.* (2014): Recent advances in understanding mTBI caused from blast loadings as well as biomechanics of TBI.[97]
10. Despotović *et al.* (2015): Methods and challenges inherent to MRI segmentation.[30]
11. Tse *et al.* (2015): Review of finite element models developed in the past decade, along with detailed listings of material properties and head injury criteria.[134]
12. Post and Hoshizaki (2015): Relation between linear and rotational accelerations on injury criteria.[114]
13. Famaey *et al.* (2015): Mechanical characteristics, constitutive models and failure criteria of bridging veins.[37]
14. Rooij and Kuhl (2016): Detailed review of constitute models proposed to model brain tissue.[120]
15. Dixit and Liu (2017): Compilation of recent developments in FE models for head injury simulations.[32]
16. Haojie Mao (2018): Introduction to anatomy of the human head in the context of head impact simulations.[94]

REFERENCES

[1]Adams, J. H., D. Doyle, D. I. GRAHMA, A. E. Lawrence, D. R. McLellan, T. A. Gennarelli, M. Pastuszko, and T. Sakamoto. The contusion index: a reappraisal in human and experimental non-missile head injury. *NNeuropathol. Appl. Neurobiol.*, 11(4):299–308, 1985.

[2]Al-Bsharat, A. S., W. N. Hardy, K. H. Yang, T. B. Khalil, S. Tashman, and A. I. King. Brain/skull relative displacement magnitude due to blunt head impact: new experimental data and model. Technical report, SAE Technical Paper, 1999.

[3]Aldrich, E. F., H. M. Eisenberg, C. Saydjari, T. G. Luerssen, M. A. Foulkes, J. A. Jane, L. F. Marshall, A. Marmarou, and H. F. Young. Diffuse brain swelling in severely head-injured children: a report from the nih traumatic coma data bank. *J. Neurosurg.* 76(3):450–454, 1992.

[4]Alshareef, A., J. S. Giudice, J. Forman, R. S. Salzar, and M. B. Panzer. A novel method for quantifying human in situ whole brain deformation under rotational loading using sonomicrometry. *J. Neurotrauma* 35(5):780–789, 2018.

[5]Arbogast, K. B., and S. S. Margulies. Material characterization of the brainstem from oscillatory shear tests. *J. Biomech.* 31(9):801–807, 1998.

[6]Arbogast, K. B., K. L. Thibault, B. S. Pinheiro, K. I. Winey, and S. S. Margulies. A high-frequency shear device for testing soft biological tissues. *J. Biomech.* 30(7):757–759, 1997.

[7]Arfanakis, K., V. M. Haughton, J. D. Carew, B. P. Rogers, R. J. Dempsey, and M. E. Meyerand. Diffusion tensor mr imaging in diffuse axonal injury. *Am. J. Neuroradiol.* 23(5):794–802, 2002.

[8]Baeck, K., J. Goffin, and J. V. Sloten. The use of different csf representations in a numerical head model and their effect on the results of fe head impact analyses. In *European LS-DYNA Users Conference 2011. Proceedings 8th European LS-DYNA Users Conference, Strasbourg, France*, 2011.

[9]Bain, A. C., and D. F. Meaney. Tissue-level thresholds for axonal damage in an experimental model of central nervous system white matter injury. *J. Biomech. Eng.* 122(6):615–622, 2000.

[10]Bass, C. R., M. B. Panzer, K. A. Rafaels, G. Wood, J. Shridharani, and B. Capehart. Brain injuries from blast. *Ann. Biomed. Eng.* 40(1):185–202, 2012.

[11]Bazarian, J. J., J. Mcclung, M. N. Shah, Y. T. Cheng, W. Flesher, and J. Kraus. Mild traumatic brain injury in the United States, 1998–2000. *Brain Inj*. 19(2):85–91, 2005.
[12]Belytschko, T., J. Fish, and B. E. Engelmann. A finite element with embedded localization zones. *Comput. Methods Appl. Mech. Eng*. 70(1):59–89, 1988.
[13]Bilston, L. E., Z. Liu, and N. Phan-Thien. Large strain behaviour of brain tissue in shear: some experimental data and differential constitutive model. *Biorheology* 38(4):335–345, 2001.
[14]Bradshaw, D. R. S., and C. L. Morfey. Pressure and shear response in brain injury models. In *Proceedings of the 17th international technical conference on the enhanced safety of vehicles, Amsterdam, The Netherlands*, 2001.
[15]Budday, S., G. Sommer, C. Birkl, C. Langkammer, J. Haybaeck, J. Kohnert, M. Bauer, F. Paulsen, P. Steinmann, E. Kuhl, et al. Mechanical characterization of human brain tissue. *Acta Biomater*. 48:319–340, 2017.
[16]Bullock, R., and D. I. Graham. Non-penetrating injuries of the head. *Cooper GJ, Dudley HAF, Gann DS et al Scientific Foundations of Trauma. Butterworth Heinemann*, pp. 101–126, 1997.
[17]Centers for Disease Control Prevention, et al. Report to Congress on Mild Traumatic Brain Injury in the United States: Steps to Prevent a Serious Public Health Problem. Atlanta, GA: Centers for Disease Control and Prevention, p. 45, 2003.
[18]Chafi, M. S., V. Dirisala, G. Karami, and M. Ziejewski. A finite element method parametric study of the dynamic response of the human brain with different cerebrospinal fluid constitutive properties. *Proc. Inst. Mech. Eng. H* 223(8):1003–1019, 2009.
[19]Chatelin, S., A. Constantinesco, and R. Willinger. Fifty years of brain tissue mechanical testing: from in vitro to in vivo investigations. *Biorheology* 47(5-6):255–276, 2010.
[20]Chatelin, S., C. Deck, F. Renard, S. Kremer, C. Heinrich, J.-P. Armspach, and R. Willinger. Computation of axonal elongation in head trauma finite element simulation. *J. Mech. Behav. Biomed. Mater*. 4(8):1905–1919, 2011.
[21]Chen, Y., and M. Ostoja-Starzewski. Mri-based finite element modeling of head trauma: spherically focusing shear waves. *Acta Mech*. 213(1-2):155–167, 2010.
[22]Chen, Y., B. Sutton, C. Conway, S. P. Broglio, and M. Ostoja-Starzewski. Brain deformation under mild impact: Magnetic resonance imaging-based assessment and finite element study. *Int. J. Numer. Anal. Model. B* 3(1):20–35, 2012.
[23]Cheng, S., E. C. Clarke, and L. E. Bilston. Rheological properties of the tissues of the central nervous system: a review. *Med. Eng. Phys*. 30(10):1318–1337, 2008.
[24]Chu, C.-S., M.-S. Lin, H.-M. Huang, and M.-C. Lee. Finite element analysis of cerebral contusion. *J. Biomech*. 27(2):187–194, 1994.
[25]Clemmer, J., R. Prabhu, J. Chen, E. Colebeck, L. B. Priddy, M. Mccollum, B. Brazile, W. Whittington, J. L. Wardlaw, H. Rhee, et al. Experimental observation of high strain rate responses of porcine brain, liver, and tendon. *J. Mech. Med. Biol*., 16(03):1650032, 2016.
[26]Cloots, R. J. H., J. A. W. Van Dommelen, S. Kleiven, and M. G. D. Geers. Multi-scale mechanics of traumatic brain injury: predicting axonal strains from head loads. *Biomech. Model. Mechanobiol*. 12(1):137–150, 2013.
[27]Cloots, R. J. H., H. M. T. Gervaise, J. A. W. Van Dommelen, and M. G. D. Geers. Biomechanics of traumatic brain injury: influences of the morphologic heterogeneities of the cerebral cortex. *Ann. Biomed.Eng*. 36(7):1203, 2008.
[28]Coats, B., S. S. Margulies, and S. Ji. Parametric study of head impact in the infant. Technical report, SAE Technical Paper, 2007.
[29]Denny-Brown, D. E., and W. R. Russell. Experimental concussion:(section of neurology). *Proc. R. Soc. Med*. 34(11):691, 1941.
[30]Despotović, I., B. Goossens, and W. Philips. Mri segmentation of the human brain: challenges, methods, and applications. *Comput. Math. Methods Med*., 2015.
[31]Destrade, M., B. M. Donald, J. G. Murphy, and G. Saccomandi. At least three invariants are necessary to model the mechanical response of incompressible, transversely isotropic materials. *Comput. Mech*. 52(4):959–969, 2013.
[32]Dixit, P., and G. R. Liu. A review on recent development of finite element models for head injury simulations. *Arch. Comput. Methods Eng*. 24(4):979–1031, 2017.
[33]Doblaré, M., J. M. Garcıa, and M. J. Gómez. Modelling bone tissue fracture and healing: a review. *Eng. Fract. Mech*. 71(13–14):1809–1840, 2004.
[34]Van Dommelen, J. A. W., T. P. J. Van der Sande, M. Hrapko, and G. W. M. Peters. Mechanical properties of brain tissue by indentation: interregional variation. *J. Mech. Behav. Biomed. Mater*. 3(2):158–166, 2010.
[35]Donnelly, B. R., and J. Medige. Shear properties of human brain tissue. *J. Biomech. Eng*. 119(4):423–432, 1997.
[36]Fallenstein, G. T., V. D. Hulce, and J. W. Melvin. Dynamic mechanical properties of human brain tissue. *J. Biomech*. 2(3):217–226, 1969.
[37]Famaey, N., Z. Y. Cui, G. U. Musigazi, J. Ivens, B. Depreitere, E. Verbeken, and J. Vander Sloten. Structural and mechanical characterisation of bridging veins: A review. *J. Mech. Behav. Biomed. Mater*. 41:222–240, 2015.
[38]Faul, M., M. M. Wald, L. Xu, and V. G. Coronado. Traumatic brain injury in the united states; emergency department visits, hospitalizations, and deaths, 2002–2006, 2010.
[39]Feng, Y., C.-H. Lee, L. Sun, S. Ji, and X. Zhao. Characterizing white matter tissue in large strain via asymmetric indentation and inverse finite element modeling. *J. Mech. Behav. Biomed. Mater*. 65:490–501, 2017.
[40]Feng, Y., R. J. Okamoto, G. M. Genin, and P. V. Bayly. On the accuracy and fitting of transversely isotropic material models. *J. Mech. Behav. Biomed. Mater*. 61:554–566, 2016.
[41]Feng, Y., R. J. Okamoto, R. Namani, G. M. Genin, and P. V. Bayly. Measurements of mechanical anisotropy in brain tissue and implications for transversely isotropic material models of white matter. *J. Mech. Behav. Biomed. Mater*. 23:117–132, 2013.
[42]Fievisohn, E., Z. Bailey, A. Guettler, and P. VandeVord. Primary blast brain injury mechanisms: current knowledge, limitations, and future directions. *J. Biomech. Eng*. 140(2):020806, 2018.
[43]Finan, J. D., S. N. Sundaresh, B. S. Elkin, G. M. McKhann II, and B. Morrison III. Regional mechanical properties of human brain tissue for computational models of traumatic brain injury. *Acta Biomater*. 55:333–339, 2017.
[44]Franceschini, G., D. Bigoni, P. Regitnig, and G. A. Holzapfel. Brain tissue deforms similarly to filled elas-

tomers and follows consolidation theory. *J. Mech. Phys. Solids* 54(12):2592–2620, 2006.
[45]Gadd, C. W. Use of a weighted-impulse criterion for estimating injury hazard. Technical report, SAE Technical Paper, 1966.
[46]Ganpule, S., N. P. Daphalapurkar, K. T. Ramesh, A. K. Knutsen, D. L. Pham, P. V. Bayly, and J. L. Prince. A three-dimensional computational human head model that captures live human brain dynamics. *J. Neurotrauma* 34(13):2154–2166, 2017.
[47]Garimella, H. I., and R. H. Kraft. Modeling the mechanics of axonal fiber tracts using the embedded finite element method. *Int. J. Numer. Methods Biomed. Eng.* 33(5):e2823, 2017.
[48]Gasser, T. C., R. W. Ogden, and G. A. Holzapfel. Hyperelastic modelling of arterial layers with distributed collagen fibre orientations. *J. R. Soc. Interface* 3(6):15–35, 2006.
[49]Gefen, A., and S. S. Margulies. Are in vivo and in situ brain tissues mechanically similar? *J. Biomech.* 37(9):1339–1352, 2004.
[50]Gennarelli, T. A., L. E. Thibault, and D. I. Graham. Diffuse axonal injury: an important form of traumatic brain damage. *The Neuroscientist* 4(3):202–215, 1998.
[51]Gennarelli, T. A., L. E. Thibault, J. H. Adams, D. I. Graham, C. J. Thompson, and R. P. Marcincin. Diffuse axonal injury and traumatic coma in the primate. *Ann. Neurol.* 12(6):564–574, 1982.
[52]Gennerelli, T. A. Comparison of translational and rotational head motions in experimental cerebral concussion. In *Proceedings of 15th Stapp Car Crash Conference*, 1971.
[53]Gentry, L.R., J. C. Godersky, and B. Thompson. MR imaging of head trauma: review of the distribution and radiopathologic features of traumatic lesions. *Am. J. Roentgenol.* 150(3):663–672, 1988.
[54]Gentry, L. R., J. C. Godersky, B. Thompson, and V. D. Dunn. Prospective comparative study of intermediate-field MR and CT in the evaluation of closed head trauma. *Am. J. Roentgenol.* 150(3):673–682, 1988.
[55]Gerber, J. I., H. T. Garimella, and R. H. Kraft. Computation of history-dependent mechanical damage of axonal fiber tracts in the brain: towards tracking subconcussive and occupational damage to the brain. bioRxiv [Preprint], p. 346700, 2018.
[56]Ghajari, M., P. J. Hellyer, and D. J. Sharp. Computational modelling of traumatic brain injury predicts the location of chronic traumatic encephalopathy pathology. *Brain* 140(2):333–343, 2017.
[57]Giordano, C., R. J. H. Cloots, J. A. W. Van Dommelen, and S. Kleiven. The influence of anisotropy on brain injury prediction. *J. Biomech.* 47(5):1052–1059, 2014.
[58]Giordano, C., and S. Kleiven. Connecting fractional anisotropy from medical images with mechanical anisotropy of a hyperviscoelastic fibre-reinforced constitutive model for brain tissue. *J. R. Soc. Interface* 11(91):20130914, 2014.
[59]Giordano, C., S. Zappalà, and S. Kleiven. Anisotropic finite element models for brain injury prediction: the sensitivity of axonal strain to white matter tract inter-subject variability. *Biomech. Model. Mechanobiol.* 16(4):1269–1293, 2017.
[60]Giordano, C., and S. Kleiven. Development of an unbiased validation protocol to assess the biofidelity of finite element head models used in prediction of traumatic brain injury. Technical report, SAE Technical Paper, 2016.
[61]Giordano, C., and S. Kleiven. Evaluation of axonal strain as a predictor for mild traumatic brain injuries using finite element modeling. Technical report, SAE Technical Paper, 2014.
[62]Graham, D. I., J. H. Adams, J. A. R. Nicoll, W. L. Maxwell, and T. A. Gennarelli. The nature, distribution and causes of traumatic brain injury. *Brain Pathol.* 5(4):397–406, 1995.
[63]Gurdjian, E. S., H. R. Lissner, J. E. Webster, F. R. Latimer, and B. F. Haddad. Studies on experimental concussion relation of physiologic effect to time duration of intracranial pressure increase at impact. *Neurology* 4(9):674–674, 1954.
[64]Hardy, W. N., C. D. Foster, M. J. Mason, K. H. Yang, A. I. King, and S. Tashman. Investigation of head injury mechanisms using neutral density technology and high-speed biplanar X-ray. *Stapp Car Crash J.* 45:337–368, 2001.
[65]Hirt, C. W., A. A. Amsden, and J. L. Cook. An arbitrary lagrangian-eulerian computing method for all flow speeds. *J. Comput. Phys.* 14(3):227–253, 1974.
[66]Ho, J., and S. Kleiven. Dynamic response of the brain with vasculature: a three-dimensional computational study. *J. Biomech.* 40(13):3006–3012, 2007.
[67]Ho, J., and S. Kleiven. Can sulci protect the brain from traumatic injury? *J. Biomech.* 42(13):2074–2080, 2009.
[68]Horgan, T. J., and M. D. Gilchrist. The creation of three-dimensional finite element models for simulating head impact biomechanics. *Int. J. Crashworthiness*, 8(4):353–366, 2003.
[69]Hosey, R. R., and Y. K. Liu. A homeomorphic finite element model of the human head and neck. *Finite Elem. Biomech.* pp. 379–401, 1982.
[70]Hrapko, M., J. A. W. Van Dommelen, G. W. M. Peters, and J. S. H. M. Wismans. The mechanical behaviour of brain tissue: large strain response and constitutive modelling. *Biorheology* 43(5):623–636, 2006.
[71]Ji, S., W. Zhao, J. C. Ford, J. G. Beckwith, R. P. Bolander, R. M. Greenwald, L. A. Flashman, K. D. Paulsen, and T. W. McAllister. Group-wise evaluation and comparison of white matter fiber strain and maximum principal strain in sports-related concussion. *J. Neurotrauma* 32(7):441–454, 2015.
[72]Jin, J.-X., J.-Y. Zhang, X.-W. Song, H. Hu, X.-Y. Sun, and Z.-H. Gao. Effect of cerebrospinal fluid modeled with different material properties on a human finite element head model. *J. Mech. Med. Biol.* 15(03):1550027, 2015.
[73]Jin, X., F. Zhu, H. Mao, M. Shen, and K. H. Yang. A comprehensive experimental study on material properties of human brain tissue. *J. Biomech.* 46(16):2795–2801, 2013.
[74]Johnson, K. L., S. Chowdhury, W. B. Lawrimore, Y. Mao, A. Mehmani, R. Prabhu, G. A. Rush, and M. F. Horstemeyer. Constrained topological optimization of a football helmet facemask based on brain response. *Mater. Design* 111:108–118, 2016.
[75]Johnson, C. L., M. D. J. McGarry, A. A. Gharibans, J. B. Weaver, K. D. Paulsen, H. Wang, W. C. Olivero, B. P. Sutton, and J. G. Georgiadis. Local mechanical properties of white matter structures in the human brain. *Neuroimage* 79:145–152, 2013.
[76]Joldes, G. R., A. L. Lanzara, A. Wittek, B. Doyle, and K. Miller. Traumatic brain injury: an investigation into shear waves interference effects. In *Computational Biomechanics for Medicine*, pp. 177–186. Springer, 2016.

[77]Joumaa, H., and M. Ostoja-Starzewski. Acoustic-elastodynamic interaction in isotropic fractal media. *Eur. Phys. J. Special Top.* 222(8):1951–1960, 2013.
[78]Kalmanti, E., and T. G. Maris. Fractal dimension as an index of brain cortical changes throughout life. *In Vivo* 21(4):641–646, 2007.
[79]King, A. I., J. S. Ruan, C. Zhou, W. N. Hardy, and T. B. Khalil. Recent advances in biomechanics of brain injury research: a review. *J. Neurotrauma* 12(4):651–658, 1995.
[80]King, A. I., K. H. Yang, L. Zhang, W. Hardy, and D. C. Viano. Is head injury caused by linear or angular acceleration. In *IRCOBI Conference*, pp. 1–12. Lisbon, Portugal, 2003.
[81]Kiselev, V. G., K. R. Hahn, and D. P. Auer. Is the brain cortex a fractal? *Neuroimage* 20(3):1765–1774, 2003.
[82]Kleiven, S. Evaluation of head injury criteria using a finite element model validated against experiments on localized brain motion, intracerebral acceleration, and intracranial pressure. *IInt. J. Crashworthiness* 11(1):65–79, 2006.
[83]Kleiven, S., and W. N. Hardy. Correlation of an fe model of the human head with local brain motion: Consequences for injury prediction. *Stapp Car Crash J.* 46:123–144, 2002.
[84]Kleiven, S., and H. von Holst. Consequences of head size following trauma to the human head. *J. Biomech.* 35(2):153–160, 2002.
[85]Kleiven, S. Predictors for traumatic brain injuries evaluated through accident reconstructions. Technical report, SAE Technical Paper, 2007.
[86]Kraft, R. H., P. J. Mckee, A. M. Dagro, and S. T. Grafton. Combining the finite element method with structural connectome-based analysis for modeling neurotrauma: connectome neurotrauma mechanics. *PLoS Comput. Biol.* 8(8):e1002619, 2012.
[87]Kruse, S. A., G. H. Rose, K. J. Glaser, A. Manduca, J. P. Felmlee, C. R. Jack Jr, and R. L. Ehman. Magnetic resonance elastography of the brain. *Neuroimage* 39(1):231–237, 2008.
[88]Lindgren, S., and L. Rinder. Experimental studies in head injury. *Biophysik* 3(2):174–180, 1966.
[89]Losoi, H., N. D. Silverberg, M. Wäljas, S. Turunen, E. Rosti-Otajärvi, M. Helminen, T. M. Luoto, J. Julkunen, J. Öhman, and G. L. Iverson. Recovery from mild traumatic brain injury in previously healthy adults. *J. Neurotrauma* 33(8):766–776, 2016.
[90]MacManus, D. B., J. G. Murphy, and M. D. Gilchrist. Mechanical characterisation of brain tissue up to 35% strain at 1, 10, and 100/s using a custom-built micro-indentation apparatus. *J. Mech. Behav. Biomed. Mater.* 87:256–266, 2018.
[91]Madhukar, A., Y. Chen, and M. Ostoja-Starzewski. Effect of cerebrospinal fluid modeling on spherically convergent shear waves during blunt head trauma. *Int. J. Numer. Methods Biomed. Eng.* 33(12):e2881, 2017.
[92]Mao, H., H. Gao, L. Cao, V. V. Genthikatti, and K. H. Yang. Development of high-quality hexahedral human brain meshes using feature-based multi-block approach. *Comput. Methods Biomech. Biomed. Eng.* 16(3):271–279, 2013.
[93]Mao, H., L. Zhang, B. Jiang, V. V. Genthikatti, X. Jin, F. Zhu, R. Makwana, A. Gill, G. Jandir, A. Singh, et al. Development of a finite element human head model partially validated with thirty five experimental cases. *J. Biomech. Eng.* 135(11):111002, 2013.
[94]Mao, H. Modeling the head for impact scenarios. In *Basic Finite Element Method as Applied to Injury Biomechanics*, pp. 469–502. Elsevier, 2018.
[95]Margulies, S. S., L. E. Thibault, and T. A. Gennarelli. Physical model simulations of brain injury in the primate. *J. Biomech.* 23(8):823–836, 1990.
[96]McIlwain, H., and H. S. Bachelard. Biochemistry and the central nervous system. 1972.
[97]Meaney, D. F., B. Morrison, and C. D. Bass. The mechanics of traumatic brain injury: a review of what we know and what we need to know for reducing its societal burden. *J. Biomech. Eng.* 136(2):021008, 2014.
[98]Meaney, D. F., and D. H. Smith. Biomechanics of concussion. *Clin. Sports Med.*, 30(1):19–31, 2011.
[99]Mendis, K. K., R. L. Stalnaker, and S. H. Advani. A constitutive relationship for large deformation finite element modeling of brain tissue. *J. Biomech. Eng.* 117(3):279–285, 1995.
[100]Miller, K., and K. Chinzei. Constitutive modelling of brain tissue: experiment and theory. *J. Biomech.* 30(11-12):1115–1121, 1997.
[101]Miller, K., K. Chinzei, G. Orssengo, and P. Bednarz. Mechanical properties of brain tissue in-vivo: experiment and computer simulation. *J. Biomech.* 33(11):1369–1376, 2000.
[102]Miller, L. E., J. E. Urban, and J. D. Stitzel. Development and validation of an atlas-based finite element brain model. *Biomech. Model. Mechanobiol.* 15(5):1201–1214, 2016.
[103]Miller, L. E., J. E. Urban, and J. D. Stitzel. Validation performance comparison for finite element models of the human brain. *Comput. Methods Biomech. Biomed. Eng.* 20(12):1273–1288, 2017.
[104]Morrison III, B., H. L. Cater, C. C. B. Wang, F. C. Thomas, et al. A tissue level tolerance criterion for living brain developed with an in vitro model of traumatic mechanical loading. *Stapp Car Crash J.* 47:93, 2003.
[105]Nahum, A. M., R. Smith, and C. C. Ward. Intracranial pressure dynamics during head impact. Technical report, SAE Technical Paper, 1977.
[106]Newman, J. A., and N. Shewchenko. A proposed new biomechanical head injury assessment function-the maximum power index. Technical report, SAE Technical Paper, 2000.
[107]Ng, H. K., R. D. Mahaliyana, and W. S. Poon. The pathological spectrum of diffuse axonal injury in blunt head trauma: assessment with axon and myelin stains. *Clin. Neurol. Neurosurg.* 96(1):24–31, 1994.
[108]Nicolle, S., M. Lounis, and R. Willinger. Shear properties of brain tissue over a frequency range relevant for automotive impact situations: new experimental results. Technical report, SAE Technical Paper, 2004.
[109]Ning, X., Q. Zhu, Y. Lanir, and S. S Margulies. A transversely isotropic viscoelastic constitutive equation for brainstem undergoing finite deformation. *J. Biomech. Eng.* 128(6):925–933, 2006.
[110]Ommaya, A. K. Mechanical properties of tissues of the nervous system. *J. Biomech.* 1(2):127–138, 1968.
[111]Ommaya, A. K. and T. A. Gennarelli. Cerebral concussion and traumatic unconsciousness: correlation of experimental and clinical observations on blunt head injuries. *Brain* 97(4):633–654, 1974.
[112]Ortiz, M., Y. Leroy, and A. Needleman. A finite element method for localized failure analysis. *Comput. Methods Appl. Mech. Eng.* 61(2):189–214, 1987.

[113]Peters, G. W. M., J. H. Meulman, and A. A. H. J. Sauren. The applicability of the time/temperature superposition principle to brain tissue. *Biorheology* 34(2):127–138, 1997.
[114]Post, A., and T. B. Hoshizaki. Rotational acceleration, brain tissue strain, and the relationship to concussion. *J. Biomech. Eng.* 137(3):030801, 2015.
[115]Prange, M. T. and S. S. Margulies. Regional, directional, and age-dependent properties of the brain undergoing large deformation. *J. Biomech. Eng.* 124(2):244–252, 2002.
[116]Pudenz, R. H., and C. H. Shelden. The lucite calvariuma method for direct observation of the brain: II. cranial trauma and brain movement. *J. Neurosurg.* 3(6):487–505, 1946.
[117]Qian, L., H. Zhao, Y. Guo, Y. Li, M. Zhou, L. Yang, Z. Wang, and Y. Sun. Influence of strain rate on indentation response of porcine brain. *J. Mech. Behav. Biomed. Mater.J. Mech. Behav. Biomed. Mater.* 82:210–217, 2018.
[118]Rashid, B., M. Destrade, and M. D. Gilchrist. Mechanical characterization of brain tissue in simple shear at dynamic strain rates. *J. Mech. Behav. Biomed. Mater.* 28:71–85, 2013.
[119]Rashid, B., M. Destrade, and M. D. Gilchrist. Mechanical characterization of brain tissue in tension at dynamic strain rates. *J. Mech. Behav. Biomed. Mater.* 33:43–54, 2014.
[120]de Rooij, R., and E. Kuhl. Constitutive modeling of brain tissue: current perspectives. *Appl. Mech. Rev.* 68(1):010801, 2016.
[121]Ruan, J. S., T. Khalil, and A. I. King. Human head dynamic response to side impact by finite element modeling. *J. Biomech.Eng.* 113(3):276–283, 1991.
[122]Sabet, A. A., E. Christoforou, B. Zatlin, G. M Genin, and P. V. Bayly. Deformation of the human brain induced by mild angular head acceleration. *J. Biomech.* 41(2):307–315, 2008.
[123]Sahoo, D., C. Deck, and R. Willinger. Development and validation of an advanced anisotropic visco-hyperelastic human brain fe model. *J. Mech. Behav. Biomed. Mater.* 33:24–42, 2014.
[124]Scofield, D. E., S. P. Proctor, J. R. Kardouni, O. T. Hill, and C. J. McKinnon. Risk factors for mild traumatic brain injury and subsequent post-traumatic stress disorder and mental health disorders among united states army soldiers. *J. Neurotrauma* 34(23):3249–3255, 2017.
[125]Shatsky, S. A., D. E. Evans, F. Miller, and A. N. Martins. High-speed angiography of experimental head injury. *J. Neurosurg.* 41(5):523–530, 1974.
[126]Shaw, N. A. The neurophysiology of concussion. *Prog. Neurobiol.* 67(4):281–344, 2002.
[127]Shuck, L. Z., and S. H. Advani. Rheologioal response of human brain tissue in shear. *J. Fluids Eng. Trans. ASME* 94(4):905–911, 1972.
[128]Smith, D. H., M. Nonaka, R. Miller, M. Leoni, X.-H. Chen, D. Alsop, and D. F. Meaney. Immediate coma following inertial brain injury dependent on axonal damage in the brainstem. *J. Neurosurg.* 93(2):315–322, 2000.
[129]Takhounts, E. G., R. H. Eppinger, J. Q. Campbell, R. E. Tannous, et al. On the development of the simon finite element head model. *Stapp Car Crash J.* 47:107, 2003.
[130]Takhounts, E. G., S. A. Ridella, V. Hasija, R. E. Tannous, J. Q. Campbell, D. Malone, K. Danelson, J. Stitzel, S. Rowson, and S. Duma. Investigation of traumatic brain injuries using the next generation of simulated injury monitor (simon) finite element head model. Technical report, SAE Technical Paper, 2008.
[131]Taylor, C. A., J. M. Bell, M. J. Breiding, and L. Xu. Traumatic brain injury-related emergency department visits, hospitalizations, and deaths-united states, 2007 and 2013. *Morb. Mortal. Wkly. Rep. Surveill. Summ.* 66(9):1–16, 2017.
[132]Thibault, L. E., and T. A. Gennarelli. Brain injury: an analysis of neural and neurovascular trauma in the non-human primate. In *Association for the Advancement of Automotive Medicine (AAAM), Conference, 34th, 1990, Scottsdale, Arizona, USA*, 1990.
[133]Toma, M., and P. D. H. Nguyen. Fluid–structure interaction analysis of cerebrospinal fluid with a comprehensive head model subject to a rapid acceleration and deceleration. *Brain Inj.* 32:1576–1584, 2018.
[134]Tse, K. M., S. P. Lim, V. B. C. Tan, and H. P. Lee. A review of head injury and finite element head models. *Am. J. Eng. Technol. Soc.* 1(5):28–52, 2014.
[135]Tse, K. M., L. B. Tan, S. J. Lee, S. P. Lim, and H. P. Lee. Development and validation of two subject-specific finite element models of human head against three cadaveric experiments. *Int. J. Numer. Methods Biomed. Eng.* 30(3):397–415, 2014.
[136]Velardi, F., F. Fraternali, and M. Angelillo. Anisotropic constitutive equations and experimental tensile behavior of brain tissue. *Biomech. Model. Mechanobiol.* 5(1):53–61, 2006.
[137]Versace, J. A review of the severity index. Technical report, SAE Technical Paper, 1971.
[138]Viana, F. A. C., T. W. Simpson, V. Balabanov, and V. Toropov. Special section on multidisciplinary design optimization: metamodeling in multidisciplinary design optimization: how far have we really come? *AIAA J.* 52(4):670–690, 2014.
[139]Viano, D. C., I. R. Casson, E. J. Pellman, L. Zhang, A. I. King, and K. H. Yang. Concussion in professional football: brain responses by finite element analysis: part 9. *Neurosurgery* 57(5):891–916, 2005.
[140]Ward, C. C. and R. B. Thompson. The development of a detailed finite element brain model. Technical report, SAE Technical Paper, 1975.
[141]Willinger, R., and D. Baumgartner. Human head tolerance limits to specific injury mechanisms. *Int. J. Crashworthiness* 8(6):605–617, 2003.
[142]Willinger, R., H.-S. Kang, and B. Diaw. Three-dimensional human head finite-element model validation against two experimental impacts. *Ann. Biomed. Eng.* 27(3):403–410, 1999.
[143]Wright, R. M., A. Post, B. Hoshizaki, and K. T. Ramesh. A multiscale computational approach to estimating axonal damage under inertial loading of the head. *J. Neurotrauma* 30(2):102–118, 2013.
[144]Yan, W., and O. D. Pangestu. A modified human head model for the study of impact head injury. *Comput. Methods Biomech. Biomed. Eng.* 14(12):1049–1057, 2011.
[145]Yang, B., K.-M. Tse, N. Chen, L.-B. Tan, Q.-Q. Zheng, H.-M. Yang, M. Hu, G. Pan, and H.-P. Lee. Development of a finite element head model for the study of impact head injury. *BioMed Res. Int.*, 2014.
[146]Yang, K. H., J. Hu, N. A. White, A. I. King, C. C. Chou, and P. Prasad. Development of numerical models for injury biomechanics research: a review of 50 years of publications in the stapp car crash conference. Technical report, SAE Technical Paper, 2006.
[147]Zhang, L., K. H. Yang, R. Dwarampudi, K. Omori, T. Li, K. Chang, W. N. Hardy, T. B. Khalil, and A. I. King.

Recent advances in brain injury research: a new human head model development and validation. *Stapp Car Crash J.* 45(11):369–394, 2001.

[148]Zhang, L., K. H. Yang, and A. I. King. Comparison of brain responses between frontal and lateral impacts by finite element modeling. *J. Neurotrauma* 18(1):21–30, 2001.

[149]Zhang, L., K. H. Yang, and A. I. King. A proposed injury threshold for mild traumatic brain injury. *J. Biomech. Eng.* 126(2):226–236, 2004.

[150]Zhao, W., B. Choate, and S. Ji. Material properties of the brain in injury-relevant conditions—experiments and computational modeling. *J. Mech. Behav. Biomed. Mater.* 80:222–234, 2018.

[151]Zhao, W., J. C. Ford, L. A. Flashman, T. W. McAllister, and S. Ji. White matter injury susceptibility via fiber strain evaluation using whole-brain tractography. *J. Neurotrauma* 33(20):1834–1847, 2016.

[152]Zhao, W., and S. Ji. Parametric investigation of regional brain strain responses via a pre-computed atlas. In *IRCOBI Conference*, pp. 208–220, 2015.

[153]Zhou, C., T. B. Khalil, and A. I. King. A new model comparing impact responses of the homogeneous and inhomogeneous human brain. Technical report, SAE Technical Paper, 1995.